



**Politecnico  
di Torino**

**Politecnico di Torino**

Master of science program in  
Environmental and Land Engineering - Climate Change  
A.y. 2021 / 2022

# Biologically Available Dissolved Organic Carbon in Glacier-fed Streams during Winter

**Supervisor:**

Prof. Costantino Manes, Politecnico di Torino

**Co-supervisor(s):**

Dr. Hannes Markus Peter, École Polytechnique Fédérale de Lausanne

Prof. Tom Jan Battin, École Polytechnique Fédérale de Lausanne

**Candidate:**

Virginia Tadei

Research project carried out in the RIVER Ecosystems Research Laboratory  
École Polytechnique Fédérale de Lausanne

## Acknowledgement

I am extremely grateful to professor Tom J. Battin, for the big opportunity of taking part in this amazing project in the RIVER Ecosystem research laboratory at EPFL.

I would like to express my deepest gratitude to Dr. Hannes M. Peter for his invaluable teachings, patience and feedback.

I could not have undertaken this journey without prof. Costantino Manes, who allowed me to write this thesis to conclude my master studies at Politecnico di Torino.

I am extremely grateful to the generous support of the Swiss Army, which allowed the sampling expeditions in extreme environments with great professionalism and sympathy.

I would like to extend my sincere thanks to Dr. Nicola Deluigi, who patiently helped in the expedition organization and laboratory analysis.

A special thanks to Dr. Andrew L. Robison for his precious advices.

I am grateful to all the RIVER lab for their willingness to help in every moment and for their great inclusivity.

I am also thankful to Laetitia Monbaron from the University of Lausanne, for taking care of the dissolved ions analysis.

I would like to thanks my family for the constant support and help they unconditionally provided me to follow my interests and reach my goals.

I would like to acknowledge Giovanni for always pushing me to achieve the maximum and overcome my limits.

At least but not last, many thanks to Hannes and Nicola for saving me from freezing in site V4.

# Contents

<b>1</b>	<b>Abstract</b>	<b>1</b>
<b>2</b>	<b>Introduction</b>	<b>2</b>
2.1	Dissolved Organic Carbon . . . . .	2
2.2	Biodegradable Dissolved Organic Carbon . . . . .	3
2.3	Primary Nutritional Groups and Organic Carbon Production . . . . .	4
2.4	Microbial activity and the DOC pool . . . . .	5
2.5	Bioassays in literature . . . . .	6
2.6	Winter factors in glacier-fed streams . . . . .	7
2.7	Bacterial Carbon Content . . . . .	8
2.8	Net DOC changes - Nomenclature . . . . .	9
2.9	Climate Change challenges . . . . .	9
<b>3</b>	<b>Methods</b>	<b>11</b>
3.1	Sites & Sampling . . . . .	11
3.2	DOC bioavailability & Degradation Kinetics . . . . .	13
3.3	Bacterial Abundance, Bacterial Volume & Bacterial Carbon Content . . . . .	15
3.4	CDOM Absorbance & Principal Components Analysis . . . . .	17
<b>4</b>	<b>Results &amp; Discussion</b>	<b>19</b>
4.1	DOC and DOC bioavailability . . . . .	19
4.1.1	DOC timeseries . . . . .	20
4.1.2	Model fitting . . . . .	22
4.1.3	Net DOC variation . . . . .	24
4.1.4	Oxidizer rate . . . . .	28
4.2	Environmental Parameters affecting DOC bioavailability . . . . .	29
4.2.1	Ultraviolet Absorbance . . . . .	29
4.2.2	Principal Component Analysis . . . . .	31
4.3	Bacterial Abundance and Bacterial Carbon Contribution . . . . .	34
4.3.1	Bacterial Abundance . . . . .	35
4.3.2	Bacterial Volume . . . . .	35
4.3.3	Bacterial Carbon Content . . . . .	38
<b>5</b>	<b>Conclusions</b>	<b>40</b>
<b>6</b>	<b>Appendices</b>	<b>42</b>
<b>A</b>		<b>42</b>
<b>B</b>		<b>43</b>
<b>C</b>		<b>44</b>
<b>D</b>		<b>45</b>
<b>E</b>		<b>47</b>
<b>7</b>	<b>Bibliography</b>	<b>61</b>

## List of Figures

1	DOC pool changes . . . . .	6
	(a) Heterotrophic pathway . . . . .	6
	(b) Chemolithoautotrophic pathway . . . . .	6
2	Glacier-fed streams in winter: characteristics . . . . .	8
3	Bacterial Carbon Content and bioassays . . . . .	9
4	Sampling sites map . . . . .	11
5	Net DOC changes: net-positive or net-negative . . . . .	14
	(a) Net negative DOC balance: the BDOC . . . . .	14
	(b) Net positive DOC balance: "Negative BDOC" . . . . .	14
6	DOC bioavailability measurement procedure . . . . .	15
7	Bacterial geometry . . . . .	16
8	Bacterial Carbon Content and the DOC pool . . . . .	17
9	DOC boxplots . . . . .	20
	(a) Raw results . . . . .	20
	(b) Without outliers . . . . .	20
10	DOC timeseries . . . . .	21
11	DOC timeseries . . . . .	22
	(a) Glacier-fed streams (blue) and MQW control (black) . . . . .	22
	(b) Alpine streams . . . . .	22
12	DOC and linear model fit . . . . .	23
13	Net DOC change . . . . .	24
14	DOC relative change . . . . .	28
15	UVA <sub>254</sub> timeseries . . . . .	29
16	Regression of the DOC variability with UVA <sub>254</sub> . . . . .	30
17	SUVA <sub>254</sub> timeseries . . . . .	31
18	Principal Component Analysis . . . . .	32
19	Bacterial length pdf . . . . .	34
20	Bacterial size . . . . .	34
21	Bacterial Abundance . . . . .	35
22	Average BV at T0 . . . . .	36
23	Average BV at T14 and T28 . . . . .	37
	(a) Average BV at T14 . . . . .	37
	(b) Average BV at T28 . . . . .	37
24	Bacterial Carbon Content timeseries . . . . .	38
25	DOC and bacterial carbon content timeseries . . . . .	39
26	Regression of the BDOC variability with SUVA <sub>254</sub> . . . . .	43
27	Average bacterial volume of the sample V4 . . . . .	45
	(a) Sample V4, T0 . . . . .	45
	(b) Sample V4, T14 . . . . .	45
28	Bacterial images of sample V4 . . . . .	45
	(a) Sample V4, T0 . . . . .	45
	(b) Sample V4, T14 . . . . .	45
29	Average bacterial volume of the sample V10 . . . . .	46
	(a) Sample V10, T0 . . . . .	46
	(b) Sample V10, T14 . . . . .	46
30	Bacterial images of sample V10 . . . . .	46

(a)	Sample V10, T0 . . . . .	46
(b)	Sample V10, T14 . . . . .	46

## List of Tables

1	Microbial metabolism pathways . . . . .	5
2	Sampling sites list . . . . .	12
3	DOC concentrations . . . . .	19
4	DOC trends in glacier-fed and alpine streams . . . . .	25
5	Significant DOC variation . . . . .	26
6	DOC % change . . . . .	27
7	Variables correlations with PC1 and PC2 . . . . .	33
8	Average bacterial volume . . . . .	37
9	Bacterial Carbon Content at T0 and T28 . . . . .	38

## Acronyms

**BA** Bacterial Abundance  
**BDOC** Biologically available Dissolved Organic Carbon  
**C** Carbon  
**CH<sub>4</sub>** Methane  
**CO<sub>2</sub>** Carbon Dioxide  
**DOC** Dissolved Organic Carbon  
**DOM** Dissolved Organic Matter  
**Fe** Iron  
**GFS** Glacier-fed streams  
**GHG** Greenhouse gases  
**Mn** Manganese  
**MQW** Milli-Q water  
**NH<sub>4</sub>** Ammonium  
**NO<sub>2</sub>** Nitrogen dioxide  
**NO<sub>3</sub>** Nitrate  
**NO<sub>x</sub>** Nitrate/Nitrite  
**O<sub>2</sub>** Oxygen  
**PCA** Principal Component Analysis  
**PC1** First Principal Component  
**PC2** Second Principal Component  
**PO<sub>4</sub>** Phosphate  
**Redox** Reduction-oxidation reactions  
**rRNA** Ribosomal ribonucleic acid  
**SO<sub>4</sub>** Sulfate Ion  
**SUVA<sub>254</sub>** Specific Ultraviolet Absorbance at 254 nm  
**TBCC** Total Bacterial Carbon Content  
**UV** Ultraviolet (light)  
**UVA<sub>254</sub>** Ultraviolet Absorbance at 254 nm  
**V** Bacterial Volume

# 1 Abstract

Glacier-fed streams (GFS), as a special type of headwater streams, play an important role in the carbon cycle through the sequestration, transformation, transport, and mineralization of organic carbon. Moreover, dissolved organic carbon (DOC) impacts downstream life and is critically important for river food webs. DOC constitutes an important nutrition source for aquatic microorganisms which form the basis of lotic food webs. This thesis aimed to fill a knowledge gap on the bioavailability of DOC in glacier-fed streams during winter. Using water samples from 14 different GFS and 4 alpine streams without glacier influence, I investigated the bio-available fraction of the dissolved organic carbon (BDOC). Laboratory bioassay procedures were combined with measurements of key environmental parameter to understand their impact on the bio-available fraction of the DOC. Strikingly, significant increases in DOC over time (or "negative" BDOC) have been found to characterize glacier-fed streams in winter conditions and are hypothesized to be related to the chemolithoautotrophic organic carbon production. Finally, I estimated bacterial carbon content to quantify the fraction of DOC that enters the food web rather than being used for microbial mineralization.

## 2 Introduction

Inland waters are important contributors to the global carbon cycle by sequestering, transporting and, mineralizing organic carbon with important consequences for the climate and carbon dioxide management [1]. Streams represent the nexus (or interface) between the terrestrial and aquatic ecosystems and they deliver organic matter to the downstream environment and ultimately to the ocean [2]. Headwaters are the smallest but also the most copious streams in the fluvial networks [3]. Thus, headwaters cover a key role in the carbon cycle in aquatic ecosystems, by transporting and transforming organic carbon [4]. Organic carbon coming from headwater streams can be delivered downstream [4], influencing the primary production and respiration of the downstream microbial life and entering river food webs. Upon microbial respiration, carbon can also be released in gaseous forms [4]. Moreover, water-borne carbon fluxes are particularly responsive to climate change due to the water cycle's sensibility to climate stresses [1].

### 2.1 Dissolved Organic Carbon

In aquatic ecosystems, organic and inorganic materials are present both, in dissolved and particulate forms. They result from dissolution or weathering processes when water passes throughout the terrestrial ecosystems. Dissolved matter is typically released from chemical weathering processes and biological leaching, while particulate matter mainly originates from mechanical breakdown, often related to freezing, thawing, and erosion. Over time, microbial activity can further increase these weathering and breakdown rates. [5] Dissolved organic matter (DOM) is of fundamental importance in aquatic ecosystems due to its multiple roles. It is involved in the biogeochemical processes as pH buffer as well as a proton donor or acceptor. DOM participates in the degradation and transport of pollutants as well as in precipitation reactions [6] and it can interact with light, to affect light availability or to be sensitive to photochemical transformations.

The largest part of the organic matter present in aquatic ecosystems is the Dissolved organic matter which consists in a heterogeneous mixture of soluble organic compounds [7]. DOM microbial mineralization rates are affected by the DOM sources that can be classified as allochthonous (terrestrial), autochthonous (in-stream primary production), groundwater, and anthropogenic [8]. Along the river continuum, DOM is transformed from primarily allochthonous (in headwaters) to primarily autochthonous (in higher-order streams) [8]. Indeed, in small streams, DOM is mainly driven by inputs of terrestrial DOM from the catchment [7]. DOM contributes to greenhouse gas emissions from inland waters by being respired by microbes to carbon dioxide and, under anaerobic conditions, to methane [8]. On the other hand, DOM provides carbon, energy, and nutrients to the aquatic ecosystem and microbial respiration [8] and accounts for a significant fraction of the organic carbon, which is taken up by heterotrophic microorganisms [2]. DOM performs other important functions, such as the attenuation of light in the water column, the link and transport of metals and other organic pollutants, and it provides a substantial contribution of the total nutrient load [8]. Technically, Dissolved organic carbon is defined as the carbon fraction of the dissolved organic matter, that passes a glass-fiber filter of 0,7  $\mu\text{m}$  nominal pore size. The DOC is a crucial regulator of aquatic metabolism [9] and the most important intermediary in the global carbon cycle [10]. It also plays a key role in aquatic food webs. By entering the microbial loop, it provides energy and carbon sources to the microbial metabolism constituting the main nutrition source for aquatic microbes [11]. It affects the primary production and, by attenuating light and affects the optical properties of the water and photo-chemical reactions. However, these multiple interactions and

chemical complexity of the DOC pool makes it difficult to predict the reactivity of DOC in aquatic ecosystems [6].

The origin of the organic carbon compounds is mainly given by the degradation of dead organic matter such as aquatic and terrestrial plants, algae, and soils. DOC can originate both, inside the water body (autochthonous DOC) and outside (allochthonous DOC). Moreover, the dissolved organic carbon is capable of hydrologically moving the carbon among the different pools [12] and it links the terrestrial and the aquatic ecosystems during its travel through the riverine environment. DOC is made up of a complex mix of molecules coming from different types of sources and subjected to multiple transformations. To obtain the dissolved organic carbon out of the organic matter pool present in the water, it is necessary to remove all the particles and large cells that constitute the particulate organic matter by using filters with nominal pore size in the order of the  $\mu\text{m}$ . However, not all of this material is bio-available.

## 2.2 Biodegradable Dissolved Organic Carbon

The biodegradable dissolved organic carbon (BDOC) is the fraction of dissolved organic carbon that can be metabolized by bacteria [13] and it can be assessed by the measurement of DOC over time. Organic carbon molecules vary in size, molecular weight, chemical bonds, element ratios, and condensation states [14]. All of these properties influence the time and energy necessary to degrade and transform the DOC molecules which can vary from minutes to millennia [14]. Overall, DOC biodegradability is a function of time that bacteria necessitate to degrade organic carbon [11]. However, there are different factors affecting organic carbon biodegradability other than the residence time of the molecules in the environment. First, intrinsic chemical properties can render DOC labile. Labile DOC describes DOC that is readily degraded by microorganisms (mainly heterotrophic bacteria) and that rapidly turns over (order of days). Recalcitrant DOC, in contrast, encompasses carbon molecules that resist microbial degradation and thus remain in the environment for a long time (from weeks and months to centuries and millennia) [14]. Typically, biodegradation leads to the rapid loss of labile and low molecular weight material [15]. However, simultaneously, production of high molecular weight aromatic compounds can be driven by heterotrophic activity [15]. The chemical composition affects the bioavailability of the DOM [16] and bacteria prefer labile molecules and, after a few days or weeks, when only larger and recalcitrant molecules are available, biodegradability continues at lower rates. This phenomenon, has been described as the reactivity continuum of DOC [17]. However, there is a debate on a possible effect, called priming effect, by which, thanks to microbial communities interaction and changes in their functionalities, the degradation of a more recalcitrant DOM pool in aquatic ecosystems, can be enhanced by the presence of labile carbon [18], resulting in higher rates of microbial remineralization [16]. Basically, microorganisms are thought to utilize energy derived from labile carbon consumption for the synthesis of enzymes capable of recalcitrant carbon breakdown. In summary, the chemical complexity of DOC and its reactivity have been intensively studied in aquatic and terrestrial environments and BDOC is now recognized as an important driver of ecosystem metabolism [9].

However, not only the chemical makeup of DOC molecules can affect the DOC biodegradability, but also the type of bacteria involved, ecophysiological features such as various uptake mechanisms, the co-acquisition or limitation by inorganic nutrients such as of phosphorus and nitrogen, complex and dynamic carbohydrate and lipid metabolism, and even bacterial motil-

ity [14]. The microbial metabolism and thus, also microbial growth, can be limited by energy, organic and inorganic nutrients [19], trace elements, and vitamins availability, that, in winter conditions of glacier environments, can be poor, affecting and limiting the biodegradation of DOC [19].

In BDOC bioassays, DOC concentration is measured at specific time intervals and the decrease in DOC concentration is modeled using linear or first-order kinetics. There are similar bio-assay procedures, such as the biological oxygen demand test, commonly used to assess waste-water purification [13]. However, the biological oxygen demand test is not suggested for drinking water or microbial ecology tests due to a deficiency in both sensitivity and specificity [13]. Sterilization techniques such as autoclaving or pasteurization are excluded, due to the possible biodegradability alteration and thus, sterilization by filtration is often preferred [13]. In this project, incubation experiments were carried out for BDOC measurements as a simple way to assess microbial organic carbon uptake and mineralization [9]. To prepare for the incubations, the water samples were sterile-filtered and an inoculum of local bacteria was added to clean incubation vessels. Temporal variation in DOC concentration was monitored and, because the incubations were performed in the dark (thus minimizing photochemical transformations), attributed to bacterial activity [13]. Incubations were carried out for 28 days, such as commonly done in BDOC assays and thus reflecting the reactivity of the labile carbon pool [8]. Then, BDOC was assessed via DOC measurements at specific time intervals and by modelling the DOC loss [9], due to net bacterial production and respiration [8], using linear or first order kinetics. However, in streams, and particularly in GFS, not only DOC consuming bacteria are present, but also non-photosynthetic microbial pathways that produce organic carbon. Bioassay procedures give the net balance of both, the dissolved organic carbon consumption and production that simultaneously happen inside the incubation bottles. This means that they resolve the net DOC variation in the pool without distinguishing between newly produced and consumed carbon. Thus, it is not possible to understand the amount of carbon that is consumed due to the contribution of carbon producers.

### **2.3 Primary Nutritional Groups and Organic Carbon Production**

Usually, organic carbon is produced via photosynthesis and thus requires light. However, the absence of light does not preclude life, indeed other pathways of organic carbon production are possible and bacterial activity can develop also in the dark [20]. More in detail, depending on the energy source, microorganisms can be divided into phototrophs, those relying on light, and chemotrophs, which utilise inorganic compounds as energy source [21]. All of these energy metabolism pathways consist in oxidation-reduction (redox) reactions that allow the transfer of electrons from reduced compounds (electron donors) to more oxidized molecules (electron acceptors) [22]. During the oxidation process, the electron donor taken up from the environment can be an organic compound, in the case of organotrophy or an inorganic compound in the case of lithotrophy. To build up biomass, microbes can utilise as carbon sources both organic substances (heterotrophs) or inorganic carbon (autotrophs) [21] such as carbon dioxide. Thus, depending on energy and carbon source availability it is possible to identify different microbial groups (Table 1). In organic carbon-poor environments, such as glacier-fed streams, it may be expected to find bacteria that rely on inorganic sources of energy and carbon. Such chemolithoautotrophs do not rely on light but utilise inorganic compounds as an energy source and carbon dioxide as a carbon source. Indeed, previous work has highlighted the presence of chemolithoautotrophic bacteria in GFS [23]. For instance, sulfur-oxidizing bacteria such as *Thiobacillus sp.* or the facultative chemolithotrophic genus *Polaromonas* are commonly found

in cryospheric environments. The scarcity of soils and other sources of organic matter in the catchments of GFS, the abundance of freshly eroded mineral surfaces often rich in sulfur and iron may explain the prevalence of these chemolithoautotrophic taxa. This may be particularly true in winter, when snow and ice cover the streams and further limit light availability for photosynthetic primary production (mediated mainly by algae during short windows of opportunity in GFS, [24]) and the associated heterotrophic bacterial communities.

Table 1: Classification of organisms based on their metabolism [25]. Subdivision based on the energy source, electron donor, and carbon source subsequently.

Energy source:	→ Light → Chemical	Photo- Chemo-	-troph
Electron donor:	→ Organic → Inorganic	-organo- -litho-	
Carbon source:	→ Organic → Carbon dioxide	-hetero- -auto-	

## 2.4 Microbial activity and the DOC pool

The DOC pool in stream ecosystems is subject to continuous variation and microbial activity, participating in the organic and inorganic material turnover [26]. The main pathway for energy fixation consists of the transformation of dissolved inorganic carbon into organic matter by photosynthesis and is called gross primary production [27]. The high-quality organic matter production by microbial activity in the stream ecosystem represents an important autochthonous energy source and it enters the riverine food web and is important to downstream consumers [27], thus contributing to the longitudinal connectivity of stream ecosystems [28]. Especially in high-elevation streams, such as glacier-fed streams above the tree line [27], where the terrestrial allochthonous supply of organic matter is poor due to the surrounding environment with bare rock and little soil, the in-stream microbial contribution plays a crucial role. More in detail, heterotrophic microbes use organic compounds as energy and carbon source to produce, together with oxygen, biomass. This process reduces the DOC pool (Figure 1a). The DOM mineralization process performed by heterotrophic bacteria is a crucial contributor to the CO<sub>2</sub> emissions to the atmosphere [18]. On the other hand, while photoautotrophs need sunlight to produce organic carbon and energy [25], some microbial communities, such as chemolithoautotrophic bacteria, can be fueled by chemosynthesis without the need for light [25]. Indeed, chemolithoautotrophic bacteria may represent a primary source of carbon in alpine streams [27] and can grow in cold and oligotrophic environments [29]. Moreover, they are capable to live in extreme conditions of pH, temperature, and pressure [29]. Chemolithoautotrophs, utilize inorganic compounds from the bedrock, such as minerals, sulfur, iron, ammonia, nitrite, and manganese, as electron donor and energy source which is stored in the chemical bonds of the inorganic compounds and is then released during oxidation [29] to produce organic compounds [22] (Figure 1b). Carbon dioxide (CO<sub>2</sub>) is consumed as the carbon source to synthesize sugars and carbohydrates [29] and to ultimately release organic matter to the DOC pool. Redox chemistries related to chemosynthesis are now increasingly recognized for their impact on biogeochemical cycles as well as greenhouse gases production and cycling [22].

Here, we selected glacier-fed streams as an ecosystem where, due to the reduced availability of organic materials, chemolithoautotrophs microbes may develop. We hypothesized that these chemolithoautotrophic communities may be particularly prevalent during winter and late-winter

conditions when snow cover reduces light availability and when the onset of snow melt increases turbidity.

It has been found by the RIVER laboratory and international collaborations that, in some BDOC incubations, the final DOC concentration exceeds the initial one. By excluding phototrophic DOC production due to incubation in the darkness, this suggests that the net-increase in BDOC bioassays could be explained by the balance of chemolithoautotrophic carbon fixation and heterotrophic carbon consumption. In the literature, there is hardly any report of unchanged or increasing trends in BDOC over time. This is maybe because of a publication bias - such rather unexpected results are not as likely to be published as "positive" results that meet our expectations. This thesis focuses on identifying environments where chemolithoautotrophic carbon fixation may outweighs heterotrophic carbon consumption.

It can be interesting, in this view, to understand if chemolithoautotrophic bacteria play an important role in glacier-fed streams during winter conditions knowing that, in this type of environment, nutrients and organic compounds are scarce and darkness prevails inhibiting the autochthonous carbon production. This may be particularly important in light of climate change and the impacts that retreating glaciers and reduced snow-cover length may have for these head-water stream ecosystems and potential downstream consequences for riverine ecosystems. In particular, we hypothesized that specific geological conditions of the catchments (related to the presence of inorganic electron donors such as sulfur, manganese or iron) determine the prevalence of chemolithoautotrophic bacteria and ultimately the production of organic compounds, potentially even exceeding heterotrophic consumption and thus leading to an increase in DOC concentration over time. On the other hand, in case the heterotrophic consumption exceeds the chemolithoautotrophs' production of organic carbon, the DOC pool would show a decrease. However, it is clear that without the addition of labeled organic and inorganic carbon sources, a complete mass balance of the DOC pool can not be achieved. However, observing the DOC trends over time can help to understand the balance between heterotrophic consumption and chemolithoautotrophs production and provide first insights into when and where chemolithoautotrophic production may be particularly important for stream ecosystems.

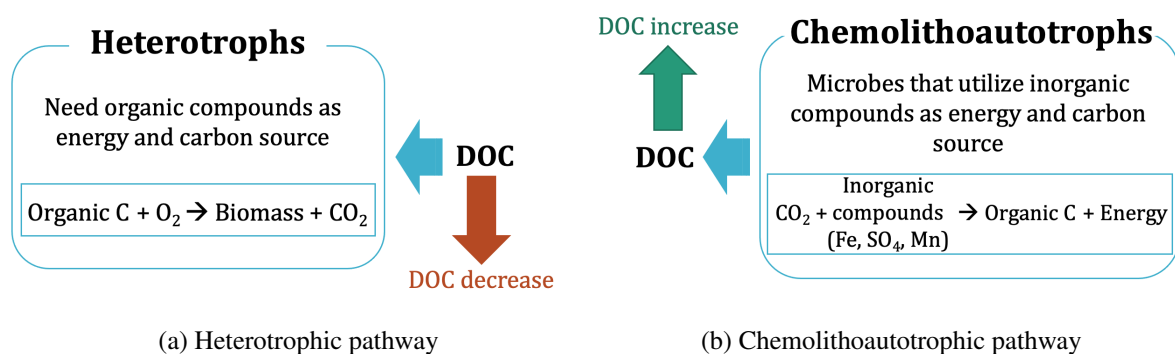


Figure 1: Heterotrophic and Chemolithoautotrophic contribution to the DOC pool of the samples. The heterotrophic metabolism consumes organic carbon coming from the DOC pool to produce biomass, decreasing the DOC pool of the sample. The chemolithoautotrophic pathway instead, utilises inorganic compounds coming from the bedrock to produce organic compounds fueling the DOC pool that increases subsequently.

## 2.5 Bioassays in literature

Dissolved organic matter loadings are also altered by human-induced or climatically induced changes that affect several ecosystems [2]. As a result, in the literature, most bio-assay pro-

cedures are done to study human impacts on freshwater ecosystems [18] [8]. For instance, land-use changes can alter the sources of freshwater DOM in Alpine fluvial network [18]. As found by Lambert et Al. , in human-disturbed waters, such as agro-urban streams, the magnitude of the DOC bio-availability [ $\text{mg L}^{-1}$ ] can account for almost double compared to forest-grassland streams with enhanced primary production and bacterial respiration [18]. In the water treatment industry, organic carbon removal is necessary to prevent bacterial growth which may cascade through trophic webs and lead to the bloom of undesired organisms [13]. Important and widespread applications of bio-assay procedures are found in wastewater management, but also analyses for drinking water purposes are carried out frequently. However, BDOC assays performed on glacial ice with an inoculum of microbes coming from glacier-fed streams, has highlighted an elevated biodegradability of DOC in glacial ice (BDOC,  $59 \pm 20\%$ ) [3] and linked this to the age of carbon in Alpine glaciers. Briefly, the notion is that ancient carbon, often derived from fossil-fuel combustion, accumulates on and within glaciers. Intense photochemical transformations at the glacier surface can break up these typically recalcitrant carbon and increase bioavailability in downstream freshwater ecosystems. However, BDOC experiments on glacier-fed streams during winter constitute a unique dataset, especially due to the glaciers' inaccessibility during winter times.

## 2.6 Winter factors in glacier-fed streams

Here, we studied glacier-fed streams as a special type of headwaters in mountainous regions under threat of climate change and ice loss, that transport and transform organic carbon to the downstream ecosystem impacting the microbial life and the entire food web. It is well known that glaciers are DOC-poor ecosystems but a significant fraction of glacier organic matter is bioavailable and plays an important role in the carbon fluxes [3]. Glacial fed-streams are extreme environments, especially during winter, when the snow cover precludes light penetration and thus, limits the autochthonous organic carbon production in the underlying water. Indeed, high levels of turbidity or snow cover in winter reduce light penetration and primary production [27]. Furthermore, the DOC delivered during winter may be highly biodegradable [19] and the organic carbon released from glacial ecosystems sustains the proglacial stream food webs to such an extent that, up to the 36% of the carbon incorporated into downstream consumer biomass is derived from the glacier ecosystem [30].

In this thesis, the focus is on glacier-fed streams during winter. Seasonality, and in this case winter conditions, apply crucial constraints to the research (Figure 2). Due to the nutrient limitation and labile DOM chemical composition, the DOC delivered in winter and early spring may be highly biodegradable [19]. Large BDOC (%) has been recorded, in some cases, in February [8] and attributed to highly biodegradable DOC mobilized during snow melt [9]. Organic nutrients are generally scarce in GFS, particularly in winter, when the soil is frozen and consequently, lateral fluxes are reduced and carbon sources are reduced. Moreover, winter flow may be dominated by groundwater, while during summer, permafrost thaw water and glacial runoff may contain larger fractions of biodegradable DOC [19]. The degradation of the antecedent summer's vegetation under snow cover during the cold season in high-alpine streams further contributes to the DOC pool [31]. Also the plant material and the atmospheric deposition within the snowpack can contribute to the DOC of the streamwater [31]. Moreover, glaciers influence the chemistry of the downstream water throughout the geochemical weathering at the glacier base [32]. All these conditions together lead to the reduced availability of organic matter in glacier-fed streams during winter, potentially, shifting the niche availability towards bacteria that can produce carbon from inorganic carbon sources. This can be the case of chemolithoau-

trophic bacteria that, as found by the NOMIS project of the EPFL's RIVER laboratory, are abundant and common in glacier-fed streams. However, winter-time analysis of BDOC coming from high altitudes streams are not widespread due to the glaciers' inaccessibility.

Here, we selected glacier-fed streams in winter as possible favorable environments for chemolithoautotrophic communities to understand, as mentioned in Section 2.4, if those bacteria are related to unchanged or increasing BDOC trends. Few alpine streams at lower altitudes have been previously analyzed using BDOC assays and even less so have attempted to determine possible drivers of net DOC changes.

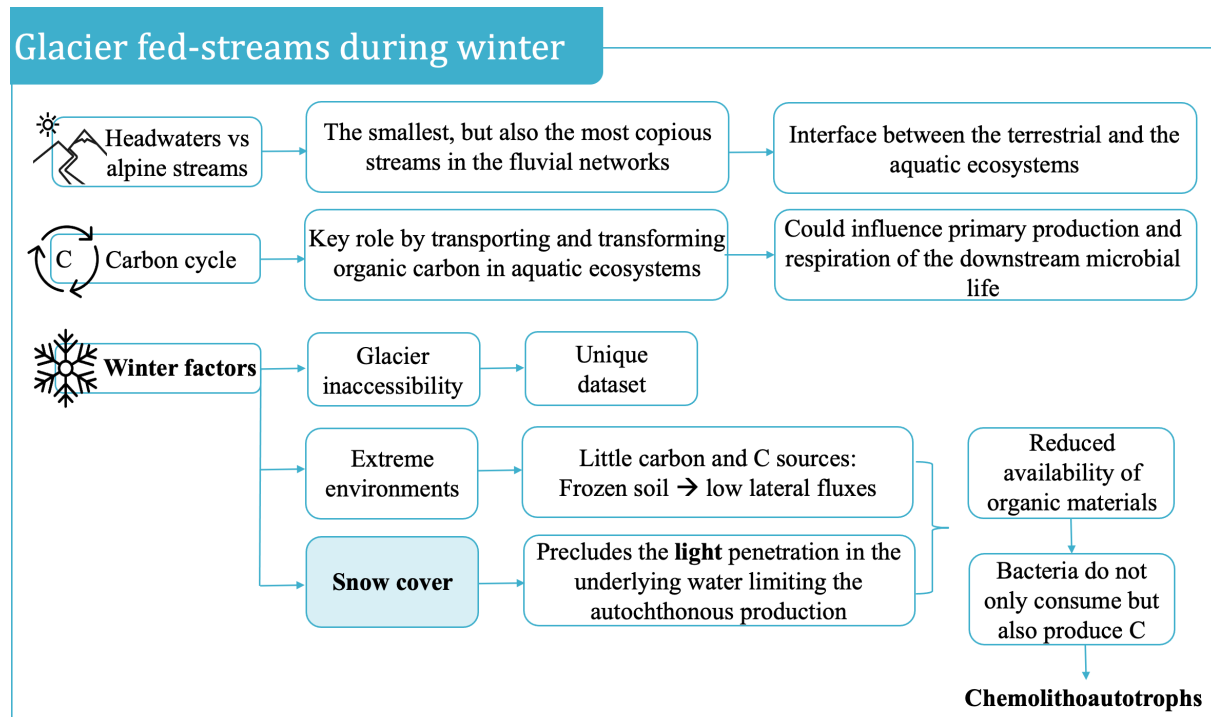


Figure 2: Key factors regulating and characterising glacier-fed streams in winter. Glacier-fed streams, as an abundant and special type of headwaters, cover a key role in the aquatic ecosystems and in the carbon cycle. Winter times in glacier-fed streams lead to the formation of an extreme environment that affects the carbon sources and the life in the streams.

## 2.7 Bacterial Carbon Content

Aquatic metabolism is highly influenced by the Dissolved Organic Carbon [9] which is degraded and taken up by microbes for respiration ( $CO_2$  production to obtain energy and inorganic nutrients) or biomass production (microbial growth). However, by accounting for the BDOC as DOC loss and without filtering the water samples before each DOC measurement, it is not possible to distinguish between the DOC that enters microbial biomass, i.e. microbial incorporation, and mineralization [19]. The predominant entry of DOM into food webs is given by the production of bacterial biomass [2] and during DOM degradation, microbes produce DOC altering, potentially, the net change in DOC concentration [19]. Therefore to track the DOC that enters biomass, bacterial abundance (BA), bacterial volume, and an literature-derived carbon content in the bacterial volume are measured and multiplied to obtain the total bacterial carbon. This procedure allowed us to track the amount of DOC that enters bacterial biomass and thus to distinguish between the effective DOC behavior and the apparent trend affected by the bacterial carbon contribution (Figure 3).

Furthermore, the nutrient balance in aquatic environments is regulated by DOM metabolism [2]. The inorganic nutrients contribute to organic forms and then the DOM pool, by supplying both respiration and primary production, can be responsible for the net ecosystem metabolism shift from heterotrophy to autotrophy [2].

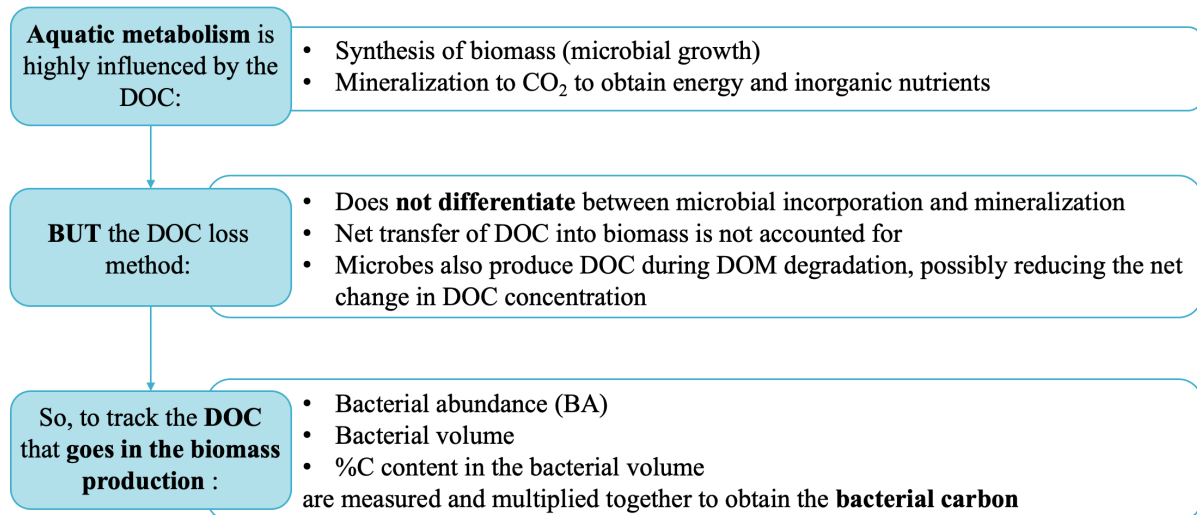


Figure 3: Bioassays do not distinguish between biomass production and mineralization but account for the net balance between them. The bacterial carbon content is further investigated to account for the DOC that is incorporated into the biomass. [19]

## 2.8 Net DOC changes - Nomenclature

Usually, BDOC assays are expected to find less DOC concentration at the end of the incubation with respect to the beginning. However, in this thesis, we measured the balance of carbon production and consumption. In the case of net-negative DOC change or, as known in literature, "BDOC" this balance is on the side of consumption, meaning that the DOC in the end is less as compared to T<sub>0</sub>. In the case of net-positive DOC change, this is on the side of production, meaning that there is more carbon in the end than in the beginning. Since the measured DOC concentration is the outcome of both production and consumption and, both increasing and decreasing net DOC changes are expected, in this thesis the "BDOC" will be referred to as "net-negative DOC change" and, for the cases in which DOC increases, "net-positive DOC change" will be used.

## 2.9 Climate Change challenges

Glaciers are sensitive environments and disappearing under unprecedented rates of climate change [27]. Downstream ecosystems are similarly under threat of global warming. A shift in the seasonality will alter those environments by decreasing snowfall events in favor of rainfall which, not only decrease the permanent glacier ice mass but will also reduce the timing and duration of snow cover and therefore ultimately the duration of ecological windows of opportunity in glacier-fed streams. Mountain streams and glacier-fed streams in particular are expected to experience more extreme hydrological regimes by shifting from high-discharge periods, due to early and faster snow melt, to seasons of drought and intermittency [27]. Thus, it is important to understand how these pristine and sensitive ecosystems will change under climate change

conditions, and how the DOC fluxes will be affected influencing the downstream life and food webs.

Carbon dioxide emissions from freshwater ecosystems can largely be attributed to terrestrial organic carbon metabolism [10] that can be enhanced by the ongoing permafrost thawing [33]. The lateral delivery of C from land to rivers has been assessed to amount between 1900 and 2700 Tg year globally [34]. Its decomposition, in high biodegradable environments, results in greenhouse gas (GHG) release (Carbon dioxide  $CO_2$  and Methane  $CH_4$ ), impacting global warming.

From a climate change perspective, global average air temperature increases, early snow-melt, and glacier retreating are leading to organic carbon mobilization [31]. Simultaneously, organic carbon previously stored in permafrost is mobilized, transported to adjacent freshwater ecosystems and there decomposed [9]. The rate and magnitude of these processes may depend on the degradability of the organic matter and properties of recipient ecosystems (e.g. limitation imposed by low temperatures or inorganic nutrient availability) which will impact the climate consequence of these processes [9] [34]. However, increasing air temperatures due to climate change have already been recognized to lead to increased DOC transport in numerous watersheds [12].

DOC concentrations and decomposition in aquatic ecosystems may be promoted, potentially impacting GHG emissions and reinforcing climate change. It has already been noted that, with glaciers retreating, the impact of mountain glaciers on the carbon cycle may change [3] as well as the impacts on glacier-fed streams [31]. Hydrological regimes, water availability, geomorphology, biodiversity, and, biogeochemistry will be altered in glacier-fed streams by organic carbon and inorganic nutrients transported with glacier runoff [31].

Thus, riverine DOC concentration and biodegradability, in response to climate warming, play a critical role in the global carbon cycle [34]. Better understanding DOC bioavailability and dynamics in freshwater ecosystems in general and in mountain stream particularly is therefore critically important. The when (winter analysis has never been done before) and where (glacier-fed streams versus alpine streams at lower altitude) of biogeochemical transformation of DOC in streams may ultimately determine if streams are sources or sinks of  $CO_2$ . Finally, the changing roles of inland waters in the global carbon cycle must be considered in order to manage and mitigate anthropogenic climate change [1].

## 3 Methods

### 3.1 Sites & Sampling

To access the glacier-fed streams along the Swiss Alps and transport water samples back to the laboratory for analysis and incubation, a Swiss Army helicopter flew us to fourteen different GFS sites at the beginning of March 2022 (Figure 4 and Table 2). Additionally, we sampled four mountain streams at lower altitude. The sites were chosen with the aim to cover a large variety of geologies of the Swiss Alps and therefore diverse redox chemistries (Table 2). The second selection criteria was determined by the need to physically find the river under the snow cover during winter time. Thus, only streams sufficiently wide not to be fully covered by the snow were selected. Third, due to the fact that glacier-fed streams are almost inaccessible during winter time at high altitudes, the helicopter support by the Swiss Army was crucial to sample the water. Thus, the locations had to be wide enough to safely allow the landing of the helicopter. Due to the fact that glacier-fed streams host very low DOC concentrations, observing DOC bioavailability trends in those samples represents a great analytical challenge. The four mountain sites at low altitude (from V15 to V18) were mainly sampled for comparison purposes. The advantages were twofold: i) to assess differences between the magnitude of DOC bioavailability in glacier-fed and mountain streams and ii) to validate the experimental procedures. Indeed, DOC bioavailability analysis in low-altitude streams are well developed and thus, they can help in the model calibration.

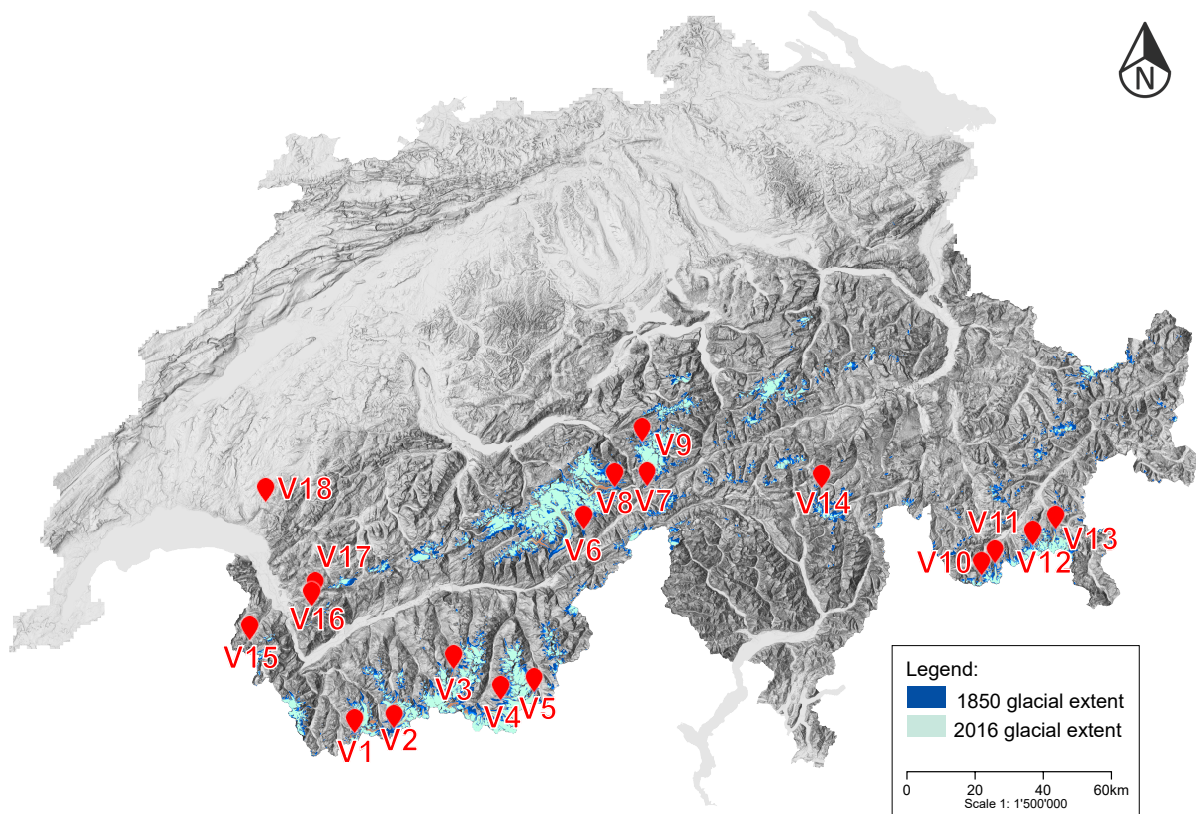


Figure 4: Map of the sampling sites along the Swiss Alps. The glaciers extent is shown in blue for the 1850 and in light-blue for the 2016, after the glacier retreat.

Table 2: Sampling sites list with their coordinates, altitude and lithology [35].

Site ID	Site Name	Coordinates (CH1903+/LV95)	Altitude (m AMSL)	Lithology
V1	Valsorey Glacier	586'149.99 mE 85'306.41 mN	3'406.7	Gneiss Micaceous Schis Prasinite Slate
V2	Otemma Glacier	598'380.94 mE 87'249.90 mN	3'474	Granodiorite Orthogneiss Eyed gneiss Mylonite
V3	Zinal Glacier	615'052.61 mE 103'545.77 mN	2'054.7	Metagranite Orthogneiss
V4	Findel Glacier	629'750.70 mE 95'505.41 mN	2'738.8	Garnet slate Mica slate
V5	Schwarberg Glacier	638'803.66 mE 97'481.95 mN	1'801.4	Gneiss
V6	Fiesch Glacier	653'450.15 mE 144'996.78 mN	2'731.5	Granite
V7	Rhône Glacier	2'671'892.251 mE 1'157'849.877 mN	3'045.6	Amphibolite Gneisses and mica slates Granite, Granodiorite Quartz diorite
V8	Unteraar Glacier	2'662'450.501 mE 1'157'653.252 mN	2'781.9	Granite Granodiorite Quartz diorite
V9	Trift Glacier	670'485.54 mE 170'853.77 mN	1'966.7	Gneiss Migmatite Amphibolite
V10	Albigna Glacier	770'009.00 mE 131'485.68 mN	2'135.5	Val Bregaglia granodiorite
V11	Forno Glacier	774'179.00 mE 134'298.04 mN	2'443.2	Val Bregaglia granodiorite
V12	Roseg Glacier	2'784'979.801 mE 1'140'550.151 mN	2'444.7	Metagranitoids Gneiss and Mica slates
V13	Morterasch Glacier	791'740.83 mE 144'656.87 mN	2'001.7	Granite Gabbro Diorite
V14	Länta Glacier	2'723'236.001 mE 1'157'165.501 mN	2'375.5	Metagranitoids Gneiss and Mica slates
V15	Champéry (Vièze)	2'555'340.022 mE 1'112'766.373 mN	1'259.3	North Helvetian flysch
V16	Avançon de Nant	2'573'560.500 mE 1'122'706.500 mN	1'187.8	North Helvetian flysch
V17	Avançon d'Anzeinde	2'574'538.603 mE 1'125'511.398 mN	1'263.2	Triassic Malm
V18	Veveyse	2'559'892.972 mE 1'153'189.136 mN	864.5	Moraine Malm

## 3.2 DOC bioavailability & Degradation Kinetics

At each site, 2 L of unfiltered stream water were collected for filtration and subsequent DOC bioavailability analysis in the laboratory (Figure 6). Moreover, at each stream, physico-chemical parameters such as water temperature, pH, electrical conductivity, barometric pressure,  $CO_2$  and  $O_2$  concentration and saturation were measured using a portable multi-meter equipped with an FDO® 925-P, a TetraCon® 925-P, a VisoTurb® 900-P and a SenTix® 940-P probe (WTW Xylem Analytics Germany) and a GMP252 probe (protected within a PTFE membrane sleeve using a handheld MI70 portable meter (Vaisala, Finland)). Also *in-situ* DOC concentration, dissolved ions and inorganic nutrients were sampled.

Due to the poor DOC concentration in glacier fed-streams, all the glass bottles (500 mL and 1 L), vials (40 mL) and pipettes (10 mL) used for the DOC analysis were acid-washed, ashed in the muffle furnace (450 °C 4 h), three-times rinsed with Milli-Q water (MQW) and three-times rinsed with the water of the sample before use, to remove any possible contamination. Also the filters were pre-combusted (450 °C for 4 h) and rinsed with Milli-Q water (MQW) and the water of the sample to avoid contamination of the bioassays (see also [13]). In the field, three replicates of stream water for Dissolved Organic Carbon (DOC) at sampling time (T0) were taken using a pre-combusted (450 °C for 4 h) glass fiber filters (GF/F grade, 0.7  $\mu$ m nominal pore size) for sterile filtration.

After the sampling, the water bottles were brought back to the laboratory within 6 hours, where the filtration of the water, for incubation purposes, took place. To remove particulate organic matter, large organisms and large bacterial cells from the samples, 1'500 ml of water of each sample were filtered through pre-combusted (450 °C for 4 h) glass fiber filters (GF/F grade, 0.7  $\mu$ m nominal pore size, 47 mm diameter). Then, with the filtered water, three replicates of 500 mL were collected in different bottles for incubation. An inoculum of 5 mL of suspended bacteria from the same site was prepared for each replicate by filtering raw samples with a pre-combusted glass fiber filter (GF/B grade, 1  $\mu$ m nominal pore size, 47 mm diameter). Then the inoculum was added to the incubation bottles. Right after the inoculum addition, the first samples were taken to obtain the initial DOC measurement at the sampling day.

The samples were incubated for 28 days at room temperature (20-22 °C) and in dark conditions, to exclude the phototrophic DOC production. By keeping all samples at the same temperature during incubation, the temperature-effects on the biological activity were removed and allowing a direct comparison of degradation kinetics between the different samples [18]. Sampling and analysis for the assays of DOC bioavailability were carried out at several time-points in order to reconstruct temporal dynamics of DOC decomposition. The first time-step consists of T0 (sampling day), followed by T2, T7, T14, T21 and T28 (i.e. 2, 7, 14, 21 and 28 days after incubation beginning). At each time point, the water was sampled from the incubation bottles with acid-washed, ashed and rinsed glass pipettes, and DOC concentration was analyzed with a Sievers M5310c TOC Analyzer (GE Analytical Instruments; accuracy:  $\pm 2\%$ , precision:  $< 1\%$ , detection limit: 22 g C/L). Using up to five injections per sample, DOC concentration was calculated as the mean of three measurements for each triplicate, excluding the lowest and the highest values.

The obtained data were analyzed using the R software and, after visual inspection, temporal DOC trends, the data were fitted using a linear model (i.e. zero-order kinetics). Only one sample of the low-altitude streams showed signs of non-linear (first-order) kinetics. To obtain DOC bioavailability values, the difference (ppb) in DOC concentration between the last time-point

of the incubation (T28) and the initial one (T0) for each site, was calculated. This was normalized to the initial DOC concentration (to obtain % difference). As outlined in Section 2.2, the bio-available fraction of dissolved organic carbon that can be metabolized by bacteria is measured throughout DOC consumption over time. This means that net-negative values of the DOC difference between T28 and T0, represent a decrease in DOC over time, the literature-known "BDOC" (Figure 5a). On the other hand, net-positive values given by the difference between T28 and T0, represent an increase in DOC over time and consequently "negative BDOC" (Figure 5b). However, the measured DOC concentrations, do not differentiate between the organic carbon which is newly produced by bacteria and the one that is consumed. In this report the "BDOC", i.e. decreases in DOC concentration over time, will be referred as "net-negative DOC change"; while the "negative BDOC", when the DOC concentrations increase, will be referred to as "net-positive DOC change". Overall, the measured DOC changes between the beginning and the end of the incubation will be mentioned as net DOC changes.

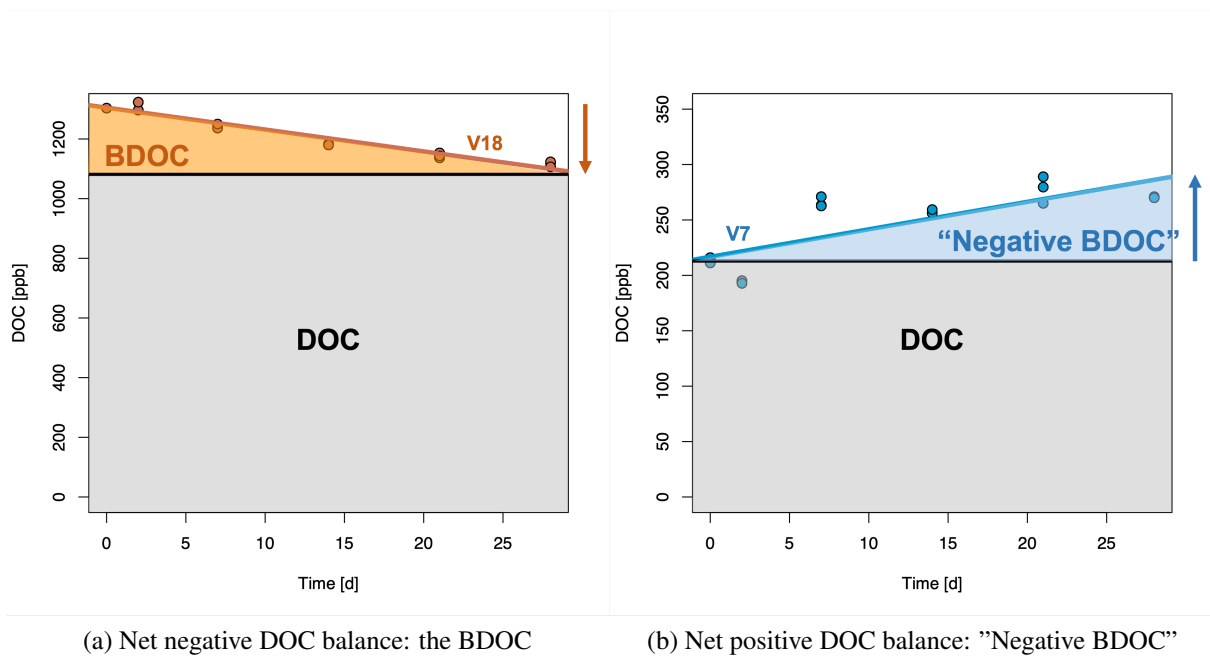


Figure 5: Net DOC balance. The net-negative DOC balance is the effective BDOC used by bacteria, here, for example, in V18, and represents the BDOC. The net-positive DOC balance is the DOC produced by bacteria and added to the DOC pool of the samples, here in V7, it can be intuitively seen as a "negative BDOC".

The net DOC change was then calculated as the difference between the final and initial DOC concentration for each replicate and the net DOC change of the sample was obtained as the average of the values coming from the three replicates of each sample:

$$\text{net DOC change} = \text{DOC}_{\text{initial}} - \text{DOC}_{\text{final}}$$

Moreover, the percent DOC change at each time-step was computed as:

$$\text{DOC}\% = (\text{DOC}_{\text{time}_i} / \text{DOC}_{\text{initial}}) \cdot \%$$

to observe the relative DOC change in time and to compare it among the samples.

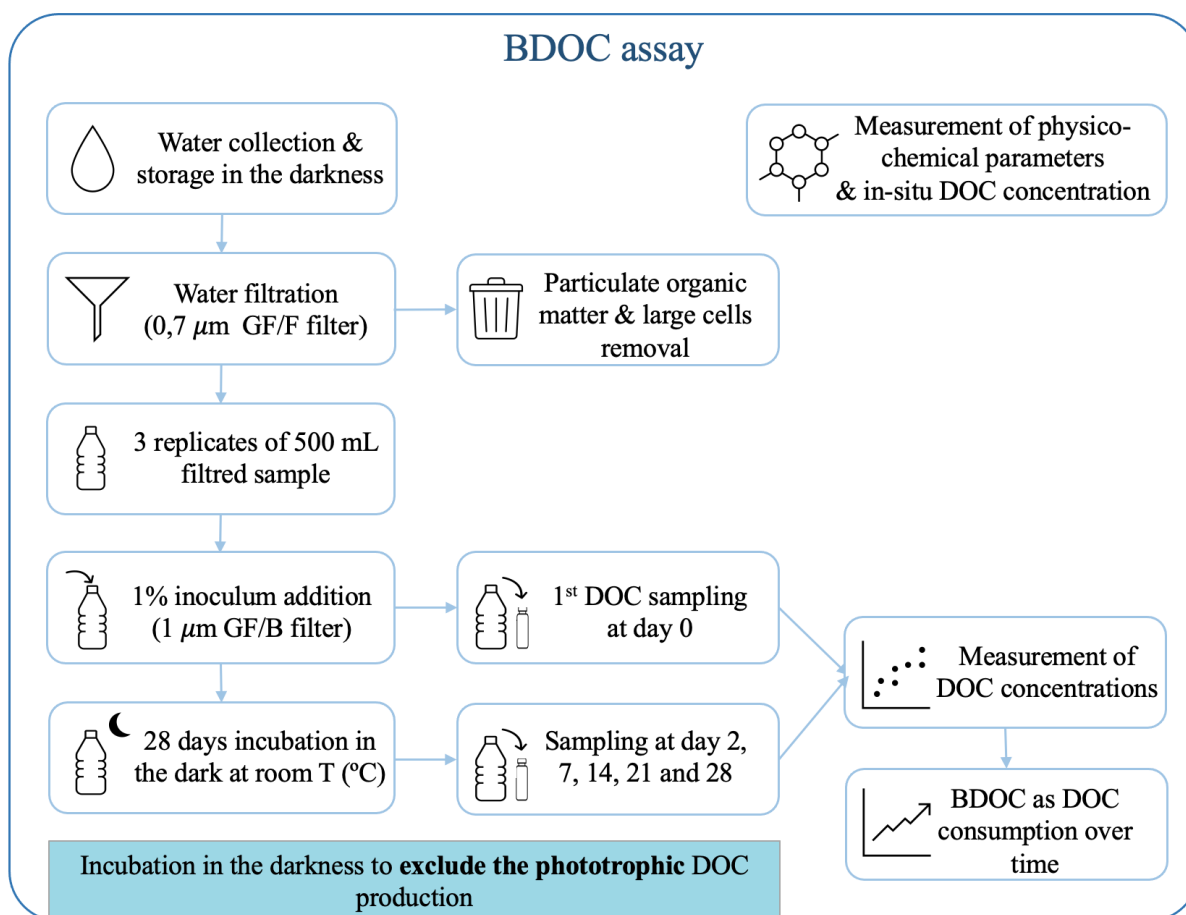


Figure 6: DOC bioavailability measurement procedure. Steps to obtain the net DOC change and its trends from the water collection. Collection of the water at the sampling sites and storage in the darkness till the laboratory analysis. Filtration of the samples (GF/F filters) to remove the particulate organic matter and large cells. Distribution of the filtered water in three bottles (500 mL) to create three replicates. Addition of 1% autochthonous inoculum (GF/B filters) in each triplicate and incubation in the darkness at room temperature to avoid the phototrophic DOC production. Sampling from the replicates and measurement of the DOC concentrations at day 0, 2, 7, 14, 21 and 28. DOC bioavailability obtained as DOC consumption over the incubation period.

### 3.3 Bacterial Abundance, Bacterial Volume & Bacterial Carbon Content

To track the microbial biomass production, bacterial abundance, average cell volume and a known percentage of carbon present in the bacterial bio-volume were measured and combined for each time-step and each sample (Figure 8). To do so, bacterial abundance (BA) was determined by flow cytometry analysis and the bacterial volume by microscope fluorescence and Microbe J analysis. To do this, simultaneously with the DOC measurements, 1.62 mL of sample were extracted from the incubation bottles, fixed with 180  $\mu\text{L}$  of a mixture of paraformaldehyde and glutaraldehyde (10% final volume) and the aliquots were immediately frozen at  $-20\text{ }^{\circ}\text{C}$  until processing within 2 months.

To prepare the flow cytometry procedure, 198  $\mu\text{L}$  of sample were added into a 96 well plate (black) and stained with 2  $\mu\text{L}$  of SYBR Green nucleic acid stain (100x solution, 1% final volume). The plates were incubated at  $37\text{ }^{\circ}\text{C}$  for 15 minutes in the dark before analysis on an Acea NovoCyte flow cytometer.

Together with the bacterial abundance, the bacterial volume was measured to investigate the

bacterial growth in time. First, fluorescence microscopy was carried out by adding to 500  $\mu\text{L}$  of the aliquots, 4  $\mu\text{L}$  of SYBR Green nucleic acid stain (100x solution) and filtration onto black polycarbonate isopore membrane filter (0.2  $\mu\text{m}$  pore size) supported by a 0.45  $\mu\text{m}$  support filter. A droplet of mounting medium for fluorescence (VectaShield) was added onto the filter before epifluorescence microscopy investigation. Using an AxioImager Z.1 (Zeiss, Germany) epifluorescence microscope (470 nm light ray, a 38 green filter and magnification 63x with oil) microphotographs of 100-200 bacterial cells per sample were taken and saved (10-20 images per sample). For bacterial length and width measurement, the microscopic images were processed using the software Microbe J, plugin in Fiji, as already done in previous studies [36].

To calculate the bacterial volume, the bacterial geometry was assumed to be cylindrical with hemispherical ends, as done previously [26]. For volume computation, the cell geometry was subdivided in three parts (Figure 7): a cylinder and two half spheres at the ends of the cylinder. The following formulas were applied:

$r = \frac{w}{2}$  where  $r$  is the half-sphere and cylinder radius and  $w$  is the bacterial width;

$V_c = \pi \cdot r^2 \cdot (L - 2r)$  where  $V_c$  is the cylinder volume and,  $L$  the bacterial length;

$V_{hs} = \frac{2}{3} \cdot \pi \cdot r^3$  where  $V_{hs}$  is the half-sphere volume;

$V = V_c + 2 \cdot V_{hs}$  where  $V$  is the bacterial volume expressed in  $\mu\text{m}^3$ .

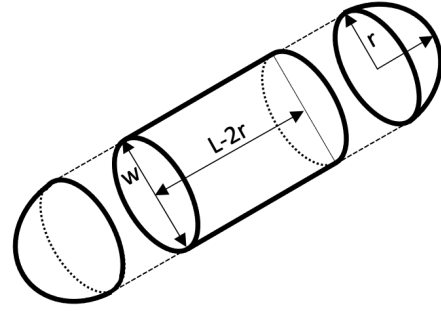


Figure 7: Bacterial geometry. Subdivision of the bacterial cell in simple shapes to calculate the bacterial volume. The bacterial geometry is subdivided in three solids: a cylinder with hemispherical ends. The radius of the cylinder, is the same of the two half spheres and consists of half cell width. To obtain the cylinder height, the radius is subtracted two times from the bacterial length. The bacterial volume is given by the sum of the cylinder volume and the two half-sphere volumes.

Obtained bacterial cell volume ranged between  $0.06 \div 0.48 \mu\text{m}^3$  and were comparable with literature-derived values ( $0.11 \div 0.41 \mu\text{m}^3$ ) [26]. Using a literature-derived conversion factor, the average carbon content per cell was estimated as:

$$\ln(C) = (1.12 \pm 0.03) \cdot \ln(V) + (4.28 \pm 0.04)$$

where  $C$  is the carbon content in fg per cell and  $V$  the measured bacterial volume in  $\mu\text{m}^3$ . Then, the carbon content per bacterial cell was multiplied with the bacterial abundance to obtain the total carbon content per sample [ $\mu\text{gL}^{-1} = \text{ppb}$ ]:

$$\text{Total Bacterial Carbon Content} = BA \cdot C$$

With the total bacterial carbon content in ppb it was possible to compare the bacterial carbon contribution to the overall DOC measured in the samples.

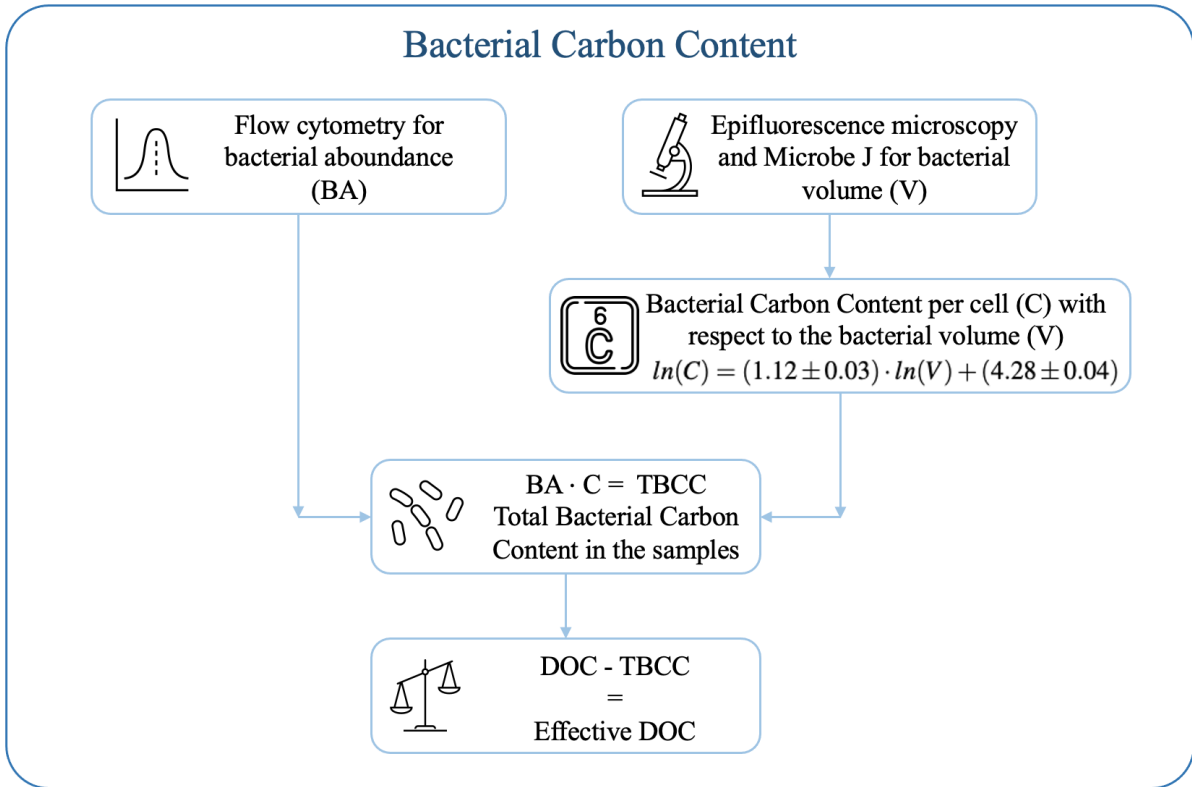


Figure 8: Bacterial Carbon Content and its contribution to the DOC pool of the samples. To obtain the effective DOC of the samples the total bacterial carbon content (TBCC) is subtracted from the overall DOC measured. The TBCC is obtained by multiplying the bacterial abundance (BA), obtained through flow cytometry, by the bacterial carbon content per cell (C). C is calculated with respect to the bacterial volume (V), obtained by epifluorescence microscopy and the Micrube J software.

### 3.4 CDOM Absorbance & Principal Components Analysis

At each time-point, in parallel to DOC bioavailability and BA analysis, the DOM optical properties were measured (UV-visible absorbance) as already done in other studies [19]. Absorption properties of colored dissolved organic matter (CDOM) were investigated by using a Perkin Elmer spectrophotometer between 200 and 800 nm of wavelength ( $\lambda$ ) and a 10 mm quartz cuvette, and were referenced to a blank spectrum of Milli-Q water. The data were then analyzed with the vegan library and R to obtain absorbance indices. Specific Ultraviolet Absorbance at ( $\lambda$ ) = 254 nm ( $SUVA_{254}$ ), is the average absorptivity of the DOC molecules in the water sample and is a proxy for relative DOC aromaticity [6] [19]. The definition of Specific UV absorbance (SUVA) rely in the absorbance of the ultraviolet light of a water sample at a given wavelength normalized for dissolved organic carbon (DOC) concentration [6] and were calculated as:

$$SUVA_{time_i} = UVA_{254time_i} / DOC_{time_i}$$

$SUVA_{254}$  is the normalized  $UVA_{254}$  index with respect to the dissolved organic carbon load in the water sample. It is positively correlated with carbon aromaticity [8].

In the field, samples of dissolved ions were collected at each site with membrane Syringe filter, Filtropur S (PES, pore size: 0.2  $\mu$ m, 33 mm diameter). The samples were then analyzed at the Institute of Earth Surface Dynamics, Faculty of Geosciences and the Environment, University of Lausanne with two 930 Compact IC Flex, Metrohm (Metrosep A Supp 7- 250/4.0,

Eluant Na<sub>2</sub>CO<sub>3</sub> 3.6 mM for the anions and Metrosep C 6- 250/4.0, Eluant HNO 6.8 mM for the cations).

Analogously, inorganic nutrient samples were collected *in situ* and immediately frozen. The nutrients (Phosphate  $PO_4$ , Ammonium  $NH_4$ , Nitrate/Nitrite  $NO_x$  and, Nitrogen Dioxide  $NO_2$  [ppb]) were then analyzed with a Hach FIA Quikchem 8500 Flow Injection Analyzer within two months after sampling. In order to run the measurements, Orthophosphate, Ammonia, Nitrate/Nitrite, Nitrite and Digestion reagents were prepared by following the protocols. Appendix A provides a list of reagents. Due to the fact that  $NO_3$  concentrations were much larger (orders of magnitude) than  $NO_2$  concentrations, it was assumed  $NO_2$  as negligible in the  $NO_x$  values and thus  $NO_3$  as representative for  $NO_x$ .

A Principal Component Analysis (PCA) was carried out on dissolved ions, inorganic nutrient, *in situ* DOC, and physio-chemical parameters to understand environmental parameters that mostly affect and drive the DOC changes. Principal Component Analysis is a dimensionality-reduction method, which allow comparison of multiple of variables with different scale-ranges in a given dataset, avoiding the excessive loss of information and accuracy. The PCA was, here, carried out in R and contained a series of steps. First, a standardization of the continuous initial variables is required, to make them contribute equally to the analysis. To get all the variables in the same scale, thanks to the "scale()" function in R, at each value of the variables, the mean is subtracted and then, everything is divided by the standard deviation:

$$z_{standardized} = (z - mean) / standard\ deviation$$

After that, a Regularized Discriminant Analysis was carried out with the "rda()" function that builds a covariance matrix to group the correlations between all the possible pairs of variables.

## 4 Results & Discussion

### 4.1 DOC and DOC bioavailability

To have a first look at the DOC concentrations and their variations among the different sites, the raw data were visualized as a boxplot for each site, by taking into consideration all three replicates (Figure 9a). From this, clear outlier were identified and removed from subsequent analyses (Figure 9b). We attribute these outliers to measurement error or contamination. DOC concentration varied widely among samples, especially when moving from glacier-fed streams (from V1 to V14) to alpine streams at lower altitudes (from V15 to V18) with some exceptions (V6, V7, V14). As expected, GFSs were characterized by low DOC concentrations, never exceeding 300 ppb; while, alpine streams at lower altitudes were characterized by higher DOC concentrations, up to an order of magnitude higher than the GFS's ones in V18. The DOC mean and standard deviation values are summarized in Table 3. Highest DOC concentration was found in V18 and it is most probably related to the low sampling altitude at 864.5 m a.s.l, compared to the other sites, that were all located above 1'188m a.s.l. At site V18, the river passed already through a valley with farmlands and alpine pastures, putatively taking up organic matter from the surrounding environment. Although higher in altitude, in the other alpine streams were still located beneath the treeline. In such the vegetated catchments, the supply of organic carbon is still high due to the contribution of both, allochthonous and autochthonous organic matter, leading to higher DOC concentrations as compared to glacier-fed streams located well above the treeline.

Table 3: DOC concentration for each sample in ppb. Given are mean and standard deviation for all replicates and time points for each sample. Outliers have been removed.

Sample	DOC (mean $\pm$ std)
V1	52.16 $\pm$ 15.76
V2	81.17 $\pm$ 25.13
V3	75.42 $\pm$ 11.06
V4	45.88 $\pm$ 8.87
V5	32.21 $\pm$ 9.84
V6	159.73 $\pm$ 11.99
V7	246.53 $\pm$ 32.56
V8	76.30 $\pm$ 13.85
V9	88.09 $\pm$ 35.47
V10	65.07 $\pm$ 13.69
V11	80.68 $\pm$ 15.93
V12	78.08 $\pm$ 13.88
V13	68.27 $\pm$ 13.20
V14	164.53 $\pm$ 6.13
V15	291.18 $\pm$ 18.99
V16	406.75 $\pm$ 13.46
V17	210.21 $\pm$ 14.05
V18	1206.04 $\pm$ 75.95

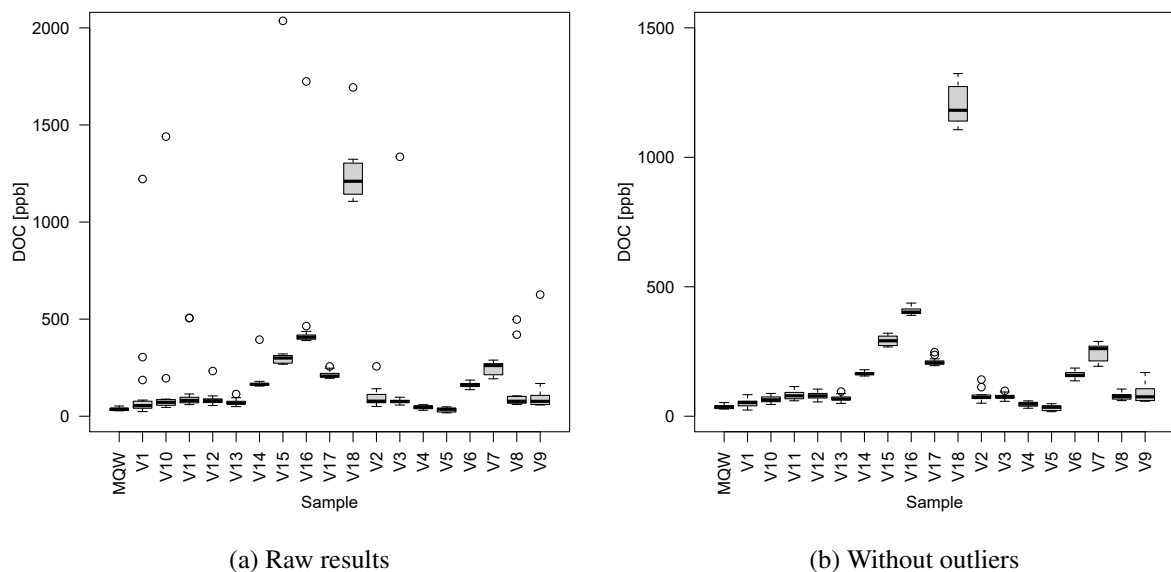


Figure 9: The two figures show boxplots of DOC concentrations [ppb] before (raw results) and after removing outliers from the dataset. Outliers were identified as  $q75 + 1.5 \times$  the interquartile range (circles in Fig. 9A). For each sample, the interquartile range (IQR) is shown as a box containing all the values between the 25th ( $Q1$ ) and 75th ( $Q3$ ) percentiles. The median value ( $Q2$ ) is highlighted by an horizontal bar in the box. Two lines, the whiskers, extending from the box, reach the minimum and maximum values given by the subtraction from  $Q1$  or the addition to  $Q3$  of a value corresponding to 1.5 times the IQR.

#### 4.1.1 DOC timeseries

After this first data processing, it was possible to investigate the timeseries of the DOC concentrations over the 28 days of incubation, avoiding biased DOC trends due to the outlier contribution (Figure 10). Here the differences in the DOC concentration between glacier-fed streams (blue, ranging from 15 to 250 ppb) and alpine streams at lower altitudes (red, ranging from 200 to 1'300 ppb) are clearly visible. These results are in line with other studies which found low DOC concentrations in glacier-fed streams of the Swiss Alps ranging between 126.7 and 207.9 ppb ( $\mu\text{g/L}$ ) [27]. The slightly lower DOC concentrations reported here may be attributable to winter conditions. However, the most interesting feature present in this figure is the slightly-increasing trend shown in most of the samples over time. This contrasts most available literature in which DOC concentrations usually decrease over time. Moreover, DOC concentrations followed a linear trend along the 28 days of incubation and, for each sample, the overall difference in DOC concentration was small, meaning little variation of DOC concentration [ppb] over time.

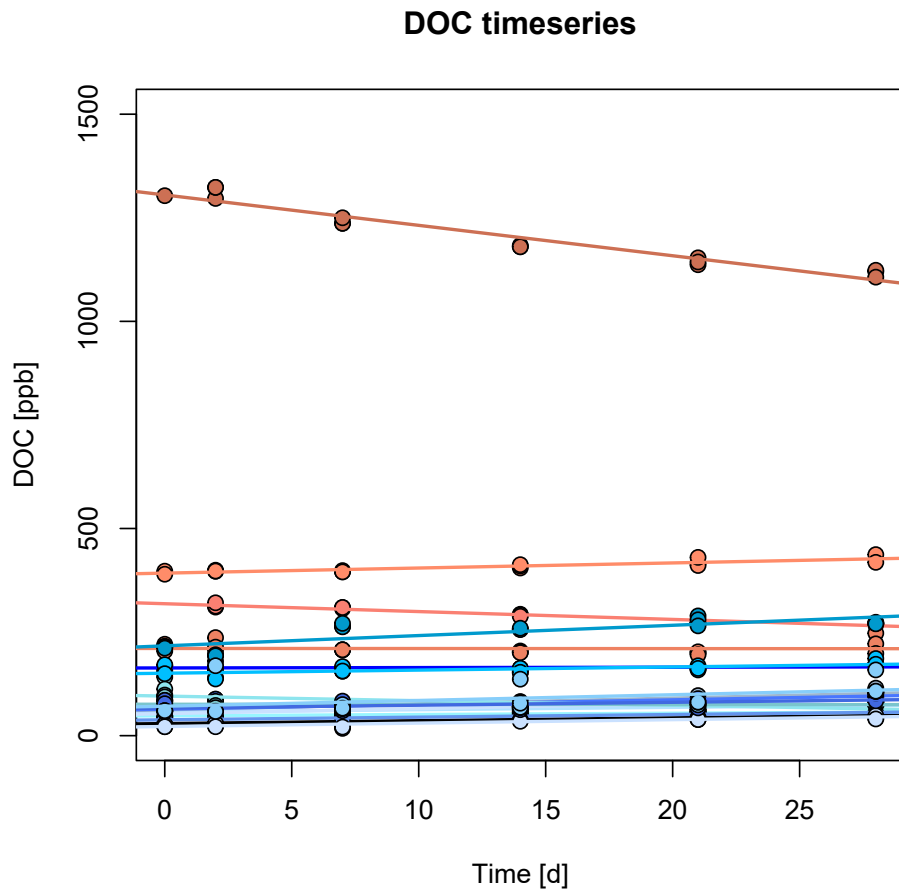


Figure 10: Timeseries of the DOC trends over 28 days among the samples. Glacier-fed streams are represented in blue colors and alpine streams in red colors. Temporal trends were obtained by fitting a linear model through the three replicated DOC measurements over time.

To better observe temporal variation, variation among the three replicates and variation among samples, the samples were next divided into glacier-fed streams (Figure 11a) and alpine streams at lower altitudes (Figure 11b). Linear models fit accurately the DOC trends in most samples over the 28 days of incubation, after excluding outliers. Strikingly, most of the GFS with DOC concentrations ranging between 20 and 100 ppb, with few exceptions up to 250 ppb, showed increasing trends in DOC over the incubation period. However, although DOC concentrations were markedly higher in alpine streams as compared to GFS streams, it is surprising that in alpine streams DOC concentrations were not always decreasing over time. Indeed, DOC concentration in these samples remained constant or even slightly increased over time in half of the samples. However, the control sample of MQW shown in black in Figure 11a, exhibited a similar increase in DOC concentration over time, comparable in relative magnitude to many of the GFSs. This fact highlights again the low carbon content of the samples coming from glacier-fed streams during winter and their small DOC variability range, which is also within the detection range of the DOC analyzer.

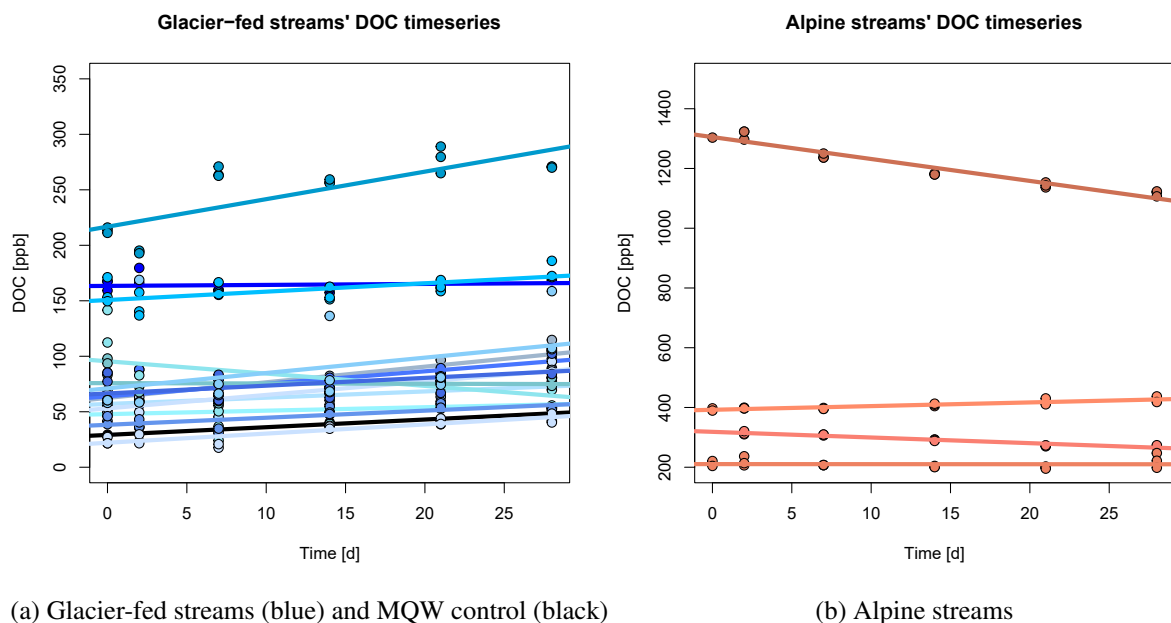


Figure 11: DOC timeseries divided in glacier-fed streams with the control sample (MQW) (11a), and alpine streams at lower altitude (11b). By looking at the two y axis range, the DOC magnitude difference between glacier-fed and alpine streams is more visible. Moreover, it is noticeable how the DOC trends behave: the general slightly increasing or flat trend in glacier-fed streams (11a) and flat or decreasing in alpine streams (11b) are characterized by concentration variability within time and replicates. Additionally the control sample of MQW shows the same DOC trend as glacier-fed streams (11a) meaning that a careful analysis of the results is needed.

#### 4.1.2 Model fitting

To visualize each sample in detail, samples were plotted individually and a linear model was fit (Figure 12). The results are based on linear regression and provide a goodness of fit for the model (adjusted  $R^2$  value) and a significance (p-value). Moreover, confidential intervals are shown to understand, together with the statistics of the model, how accurately the linear model fits the observed data. In Figure 12 it is apparent that different samples behave in different ways. In most of the cases, the DOC starting concentration was low, and its range is small, covering a few tens of ppb of variations as also highlighted by the slope gradient of the linear model ("slp" in Figure 12). Inspection of regression slopes of each sample, revealed that the DOC concentrations in glacier-fed streams increased on average by 0.7 ppb per day, while in alpine streams, on average, it decreased about 2 ppb per day (with bigger differences among the samples). The model explained well DOC variations, with a  $R^2$  lower than 0.3 in only few cases (V1, V2, V3, V8, V9, V10, V14 and, V17). Additionally, the linear model fits well in some samples, as highlighted by the p value of the model ("p" in Figure 12). Indeed, a p value lower than 0.05 means that the linear model fits statistically significant in the samples V4, V5, V6, V7, V8, V11, V12, V13, V15, V16, and V18. While, in the other cases, a linear model is not well representative of the DOC variation over time. We attribute this mainly to variation in DOC dynamics among replicates and non-linear dynamics. However, it could be interesting to explore if the linear fitting could be improved. For example, additional outliers could be identified based on linear model confident intervals and removed to see if the fitting would improve at least for some samples (for example, V9 and V17). Nevertheless, even if this procedure would improve model fits in some samples it seems far from an improvement that affects relevantly the results without compromising the representativeness of the data.

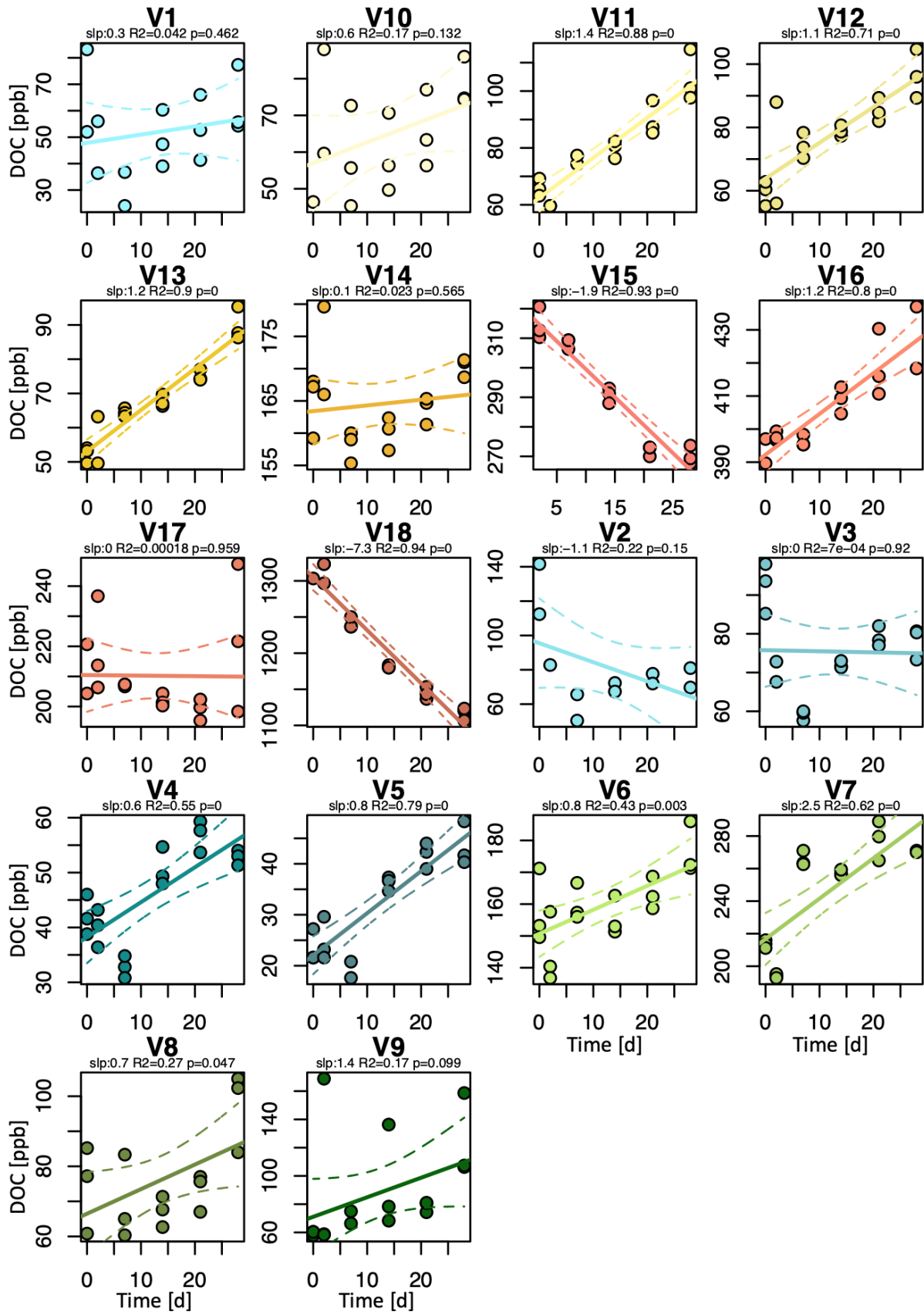


Figure 12: DOC trends of individual samples fitted by a linear model. Above each graph the statistics of the model are shown: *slp* as the slope gradient of the line and *p* value to assess the statistical significance of the model. The model slope is generally low meaning that the DOC concentrations do not vary greatly with time. Moreover, the model fits significantly the data if the *p* value is lower than 0.05, while in the other cases, such as V1, V2, V3, V9, V10, V14 and V17, the model do not fit well the data and thus it is not representative of the DOC trend.

### 4.1.3 Net DOC variation

We next looked at the magnitude of DOC bioavailability among samples. In Figure 13, the difference in ppb of the DOC concentration between the last time-point of the incubation (T28) and the initial one (T0) is plotted for each site. As stated in Section 3.2, in this study we took the difference between T28 and T0 as the net DOC change, meaning that negative values in Figure 13 represent a net-negative DOC change where the balance between bacterial production and consumption is dominated by the consumption of carbon, which is used by bacteria during the incubation. While, positive values in the same plot account for a net-positive DOC change, shifted on the production side, due to the production of newly organic carbon during the 28 days.

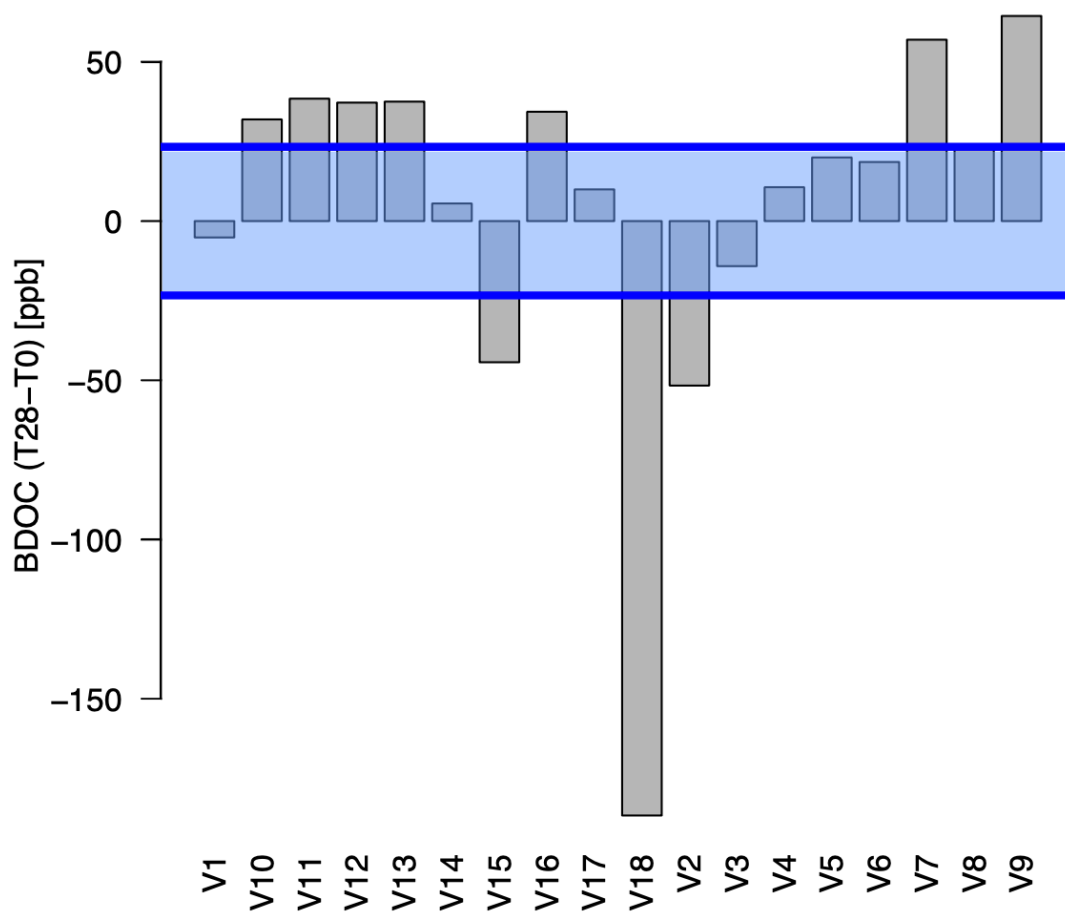


Figure 13: Net DOC change [ppb] during the 28 days of incubation for each sample. Negative values represent net-negative DOC changes (BDOC), while positive values are related to a net-positive DOC changes (or net DOC increase). The MQW's DOC variability (blue) is set as threshold for the reliability of the data: DOC changes (both positive or negative) lower than 23.33 (MQW DOC change, inside the blue bar) are considered not to be significant because of uncertainty of measurements.

As observed before, most of the samples exhibited a net positive DOC balance meaning that, probably, the bacteria present in the glacier-fed streams contribute to the DOC pool of the incubation bottles by releasing organic carbon. More in detail, out of 14 glacier-fed streams (Table 4), 11 exhibited a net-positive DOC change of the magnitude between 5 and 65 ppb ( $33.78 \pm 19.36$  ppb) over 28 days; while only 3 showed a net-negative DOC change between 5

and 50 ppb ( $23.66 \pm 24.67$  ppb) over the 28 days. In the case of alpine streams at lower altitude, 2 out of 4 sites were characterized by a net-negative DOC change ranging between 44 and 187 ppb ( $115.50 \pm 100.64$  ppb), while the other half exhibited a net-positive DOC change ranging from 10 to 44 ppb ( $22.14 \pm 17.24$  ppb) over the incubation period.

*Table 4: In both cases, glacier-fed or alpine streams, the number of samples with increasing or decreasing DOC trends and their magnitude are reported. It is noticeable that, in most of the glacier-fed streams the DOC concentration increased with time, while in only 3 cases some net-DOC decrease is found. In the case of alpine streams, both positive and negative DOC changes were evident.*

Site	N. of samples	DOC changes	Magnitude [ppb]
Glacier-fed streams	11/14	Increasing (net-positive) ↗	from 5 to 65
	3/14	Decreasing (net-negative) ↘	from 5 to 50
Alpine streams	2/4	Increasing (net-positive) ↗	from 10 to 44
	2/4	Decreasing (net-negative) ↘	from 44 to 187

However, since the DOC concentrations measured were close to the detection level of the DOC analyzer, and the control sample (MQW) increased by 23 ppb during the incubation, the reliability of the results must be carefully considered. By taking the net DOC change of the MQW as the threshold for the data reliability, significant DOC variation (Table 5) was only found for samples that exceed the MQW variation range (exceeding the blue range in Figure 13). With this conservative estimate, only a few samples exhibited significant changes in DOC concentration. Specifically, the net-negative DOC change was observed in three samples: in two alpine streams, V18 and V15, and one glacier-fed stream, V2. The significant net-negative DOC change magnitude in the three above-mentioned samples varied considerably (Table 5): from 163 ppb in V18 to 21 and 28 ppb in V15 and V2, respectively. Concerning the net-positive DOC change, a significant fraction can be accounted for V7, V9, V10, V11, V12, V13, and V16. In this case, the magnitude of significant net-positive DOC change varies between 9 and 41 ppb depending on the sample. Now, by looking back at Figure 9b, it is possible to understand if a correlation between initial DOC concentration and DOC trends is present or not. The initial DOC concentration of sample V18 was the highest of the dataset (Figure 9b) as well as its net-negative DOC change magnitude (Figure 13). However, the sample with the second highest DOC starting concentration, V16 (Figure 9b), showed a net-positive DOC change at the end of the incubation (Figure 13) up to a magnitude that can be considered reliable. Another noticeable case is V2, which has a starting DOC concentration around 100 ppb, in the range of the other glacier-fed streams, but exhibited the second highest net-negative DOC change value (Table 5) while, all the other GFSs with significant DOC variation showed an opposite trend, with a net-positive DOC change. Thus, it seems that net DOC change trends and, DOC variations in general, in mountain streams during winter may not be controlled by initial DOC concentration. This contrasts the current state of the literature [11].

Table 5: Here the samples with a significant DOC variation (greater than the MQW DOC variation) are reported with the DOC change magnitude and its significant fraction. Only three samples show a significant net-negative DOC change (BDOC), while all the others show a net-positive DOC change ranging between 8.6 and 41.18 ppb.

Sample	Net DOC change [ppb]	Significant net DOC change [ppb]
V2	-51.67	-28.34
V7	56.96	33.63
V9	64.51	41.18
V10	31.93	8.60
V11	38.44	15.11
V12	37.20	13.87
V13	37.51	14.18
V15	-44.33	-21.00
V16	34.33	11.00
V18	-186.66	-163.33

The relative DOC change is plotted in Figure 14 to compare the net DOC change after the 28 days of incubation among the samples, avoiding scale differences. Initial DOC concentration (at T0) was scaled to 100%. For most of samples, the relative change in DOC after the incubation was positive, i.e. exceeding 100%, and indicating that no DOC production exceeded or balanced DOC consumption. Moreover, the relative increase in DOC is not negligible, it reached values greater than 200% meaning that initial DOC concentrations even doubled. Yet, few samples, as already seen also in Figure 13, were characterized by a net-decreasing DOC change.

However, we found a mismatch between the magnitude of the relative DOC change and the absolute magnitude of the DOC change (in ppb). Indeed, comparing values in Table 6 and Table 5, the greatest DOC variation in ppb was not related to the greatest relative DOC change [%] and thus, biodegradability seems not to be related to the initial DOC concentration. As an example, V18 and V15 showed the same relative DOC change, about 14%, but their net negative DOC variation differed by 142 ppb (186.66 ppb for V18 and 44.33 ppb for V15). Moreover, in the case of glacier-fed streams, low DOC concentrations were related to low DOC variations in terms of ppb but the DOC % change can be high even with few ppb of variation. Thus, when comparing the percentage of net-positive DOC change of GFSs with the net-negative DOC change magnitude [%] of alpine streams at a lower altitude, the magnitude of the effective DOC change in ppb is much different and can be related to the small variability of the GFSs' DOC concentration. The highest relative DOC variation was associated to V9 with a percentage increase of 108.25% meaning that the DOC in the sample is more than doubled. Among samples with a significant DOC change (in bold in Table 6), the relative DOC change was greater in magnitude when the relative net DOC change was positive (from 26 to 108 % increase) rather than when the relative net DOC change was negative (BDOC between 14 and 41 %).

Those results differ from what was reported previously in the literature. First, no positive relative DOC changes are reported, maybe because the unexpected or "unreasonable" results are not as likely to be published. Across the global rivers, net-negative DOC change (BDOC) values between 0.1% and 72.2%, with a global mean of 16.4% of the initial concentration are found [34]. This variability is high and depends on the site location, its position along the transect, and the human impact on the water. For example, in tropical rivers, mean net-negative DOC change (BDOC) has been found around 40% [11]. In Belgian rivers, depending on the pollution level, net-negative DOC change (BDOC) can vary between 26÷54 % and 19÷34 % for

less polluted sites [13]. In subtropical to temperate and humid regions, blackwater net-negative DOC change (BDOC) ranges between 2.26 and 11.91 % [16]. In first-order Coastal Plain headwater streams the biodegradability was reported around 25% but can vary according to the urbanization level [4]. Moreover, the DOC bioavailability has been reported to be significantly greater in 1st- than 2nd-order streams in the Lamprey River watershed with a mean annual net-negative DOC change (BDOC) (%) ranging from 8.9% to 26.0% [8].

However, data about glacier-fed streams during winter are scarce. Focusing on glaciers, Fellman et Al. [30] estimated from isotopic signatures of biofilms up to 45÷83% of biodegradability in the upper Herbert River. However, the 20÷80% [3] and 50% [30] of DOC bioavailability estimated by laboratory bioassays refer to glacier ice and melt water originating from glaciers but not to the glacier-fed stream waters.

In Swiss catchments, net-negative DOC change (BDOC) has been found by Lambert et Al. [18] to range between 9.7 and 57.6% of initial DOC (mean=33.8±11%) with higher values in agro-urban streams. Net-negative DOC change (BDOC) ranged on the order of ppm in the report [18], which is one or two orders of magnitude greater than in the glacier-fed streams of this study. However, the sampling sites are located at lower altitudes and do not include glacier-fed streams. Overall, glacier-fed streams during winter show DOC trends and net DOC changes that highly differ from the literature. Indeed, looking at Figure 14, it is well visible that most of the samples have net DOC change values out of the range of values known from literature. This is not surprising given the extreme nature of these environments and the scarcity of allochthonous and autochthonous carbon sources. While

this may be the case for GFS in general, it may be even more enhance because of the "special" conditions that characterize glacier-fed streams during winter, such as the frozen soil, the absence of light and the reduced sources of organic carbon. Moreover, a large quantity of the carbon trapped in glacier ecosystems may be photo-degraded ancient carbon which is not available during winter but only when the snow melts and thus it enters the fluvial ecosystems during the warm period, leading to the measurement of higher DOC concentrations.

Table 6: Percentage variation of the DOC in the samples. The samples with significant DOC change are in bold.

Sample	DOC change %
V1	-7.62
<b>V2</b>	<b>-40.68</b>
V3	-15.34
V4	25.27
V5	85.12
V6	11.74
<b>V7</b>	<b>26.67</b>
V8	30.52
<b>V9</b>	<b>108.25</b>
<b>V10</b>	<b>68.81</b>
<b>V11</b>	<b>58.24</b>
<b>V12</b>	<b>62.56</b>
<b>V13</b>	<b>71.78</b>
V14	3.36
<b>V15</b>	<b>-14.09</b>
<b>V16</b>	<b>8.73</b>
V17	4.68
<b>V18</b>	<b>-14.32</b>

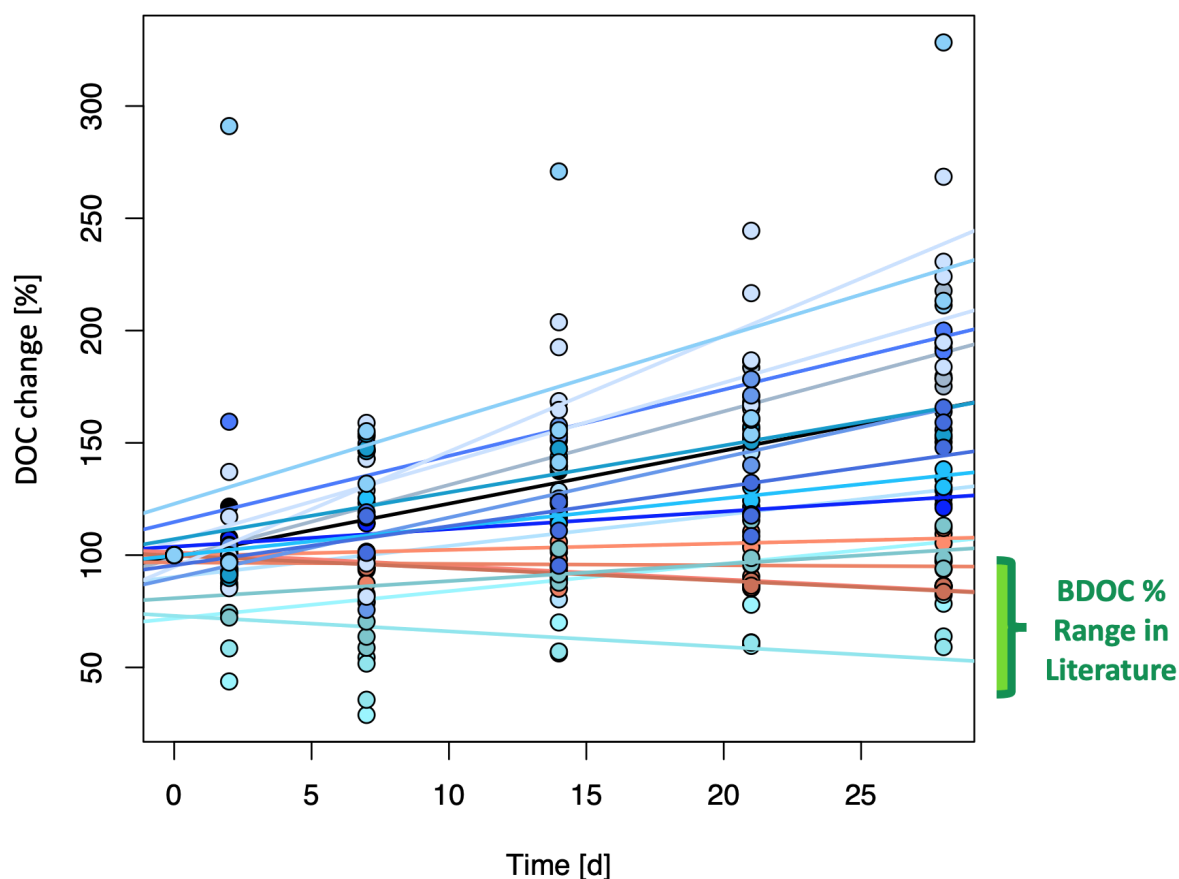


Figure 14: Relative DOC change. The initial DOC concentration is set at 100% and the DOC change in time is relative to it. Most of the samples show a net DOC [%] increase meaning that no BDOC is shown. Only few samples (V2, V15 and V18) lead to net-negative DOC measurements that fit the BDOC literature range.

#### 4.1.4 Oxidizer rate

V2 showed the second highest net-negative DOC change [ppb] and it is the only glacier-fed stream that shows some net-decreasing DOC change during the incubation experiment. This result is probably not reliable because at T0 and T2 high oxidizer rates were injected in the sample due to a DOC machine malfunction. Indeed, during the DOC measurement, the DOC analyzer injects acid and oxidizer at a given rate [ $\mu\text{L}/\text{min}$ ] depending on the detected DOC concentration. In the case of MQW, the acid rate is fixed at  $2 \mu\text{L}/\text{min}$  and the oxidizer rate at  $0 \mu\text{L}/\text{min}$  to allow the redox reactions during the DOC analysis. In glacier-fed stream samples, the DOC concentrations are close to the MQW ones and the injected rates, which are set as automatically chosen by the machine are expected to be close as well. At the beginning of the DOC analysis (T0 and T2), the oxidizer rate pipe was malfunctioning due to the presence of a small air bubble, likely leading to an underestimation of the DOC concentration [ppb] by about 20%. After quantifying this error using standards in the DOC analyzer, this problem was overcome by adjusting the results adding the missing 20 % of DOC. However, when the rate of injected oxidizer in the sample was too high (exceeding  $0.3 \mu\text{L}/\text{min}$ ), the measured DOC concentration was much higher than the one measured without oxidizer, up to a shift in magnitude from ppb to ppm. In some cases, this problem was affecting only one replicate and its exclusion from the dataset was sufficient to fix the problem. In the case of V2 however, this problem was persistent in all triplicates at both T0 and T2, leading to a biased result. Hence, V2 should be excluded from the analysis.

## 4.2 Environmental Parameters affecting DOC bioavailability

### 4.2.1 Ultraviolet Absorbance

The absorbance of the UV light by DOC molecules provides information on the molecular composition and can be related to DOC reactivity [6]. Indeed, in aquatic ecosystems, DOC biodegradability is affected and driven by the chemical composition of the molecules [19]. In the near UV spectra ( $\lambda = 200\div 380$  nm) specific molecular arrangements, such as the presence of aromatic molecules, absorb most of the radiation [6]. The  $UVA_{254}$  index represents the light absorbed by organic compounds, especially the aromatic ones, in a water sample. Light at 254 nm is absorbed by the organic molecules present in the water and thus, absorption at 254 nm is of particular interest and provides information about the organic matter composition.

The  $UVA_{254}$  index showed an increasing trend over time in all the samples (Figure 15). In general, it increased until T14, then it dropped at T21, to increase again until the end of the incubation. Higher  $UVA_{254}$  values characterized the alpine streams at lower altitudes (V15, V16, V17, V18), and glacier-fed streams with elevated DOC concentrations compared to the other samples (V6, V7, V14). However, it was noticeable that, even when no net-negative DOC change (BDOC) was found in the samples, the  $UVA_{254}$  index increased, indicating that microbial activity acted on the DOM in the bioassays.

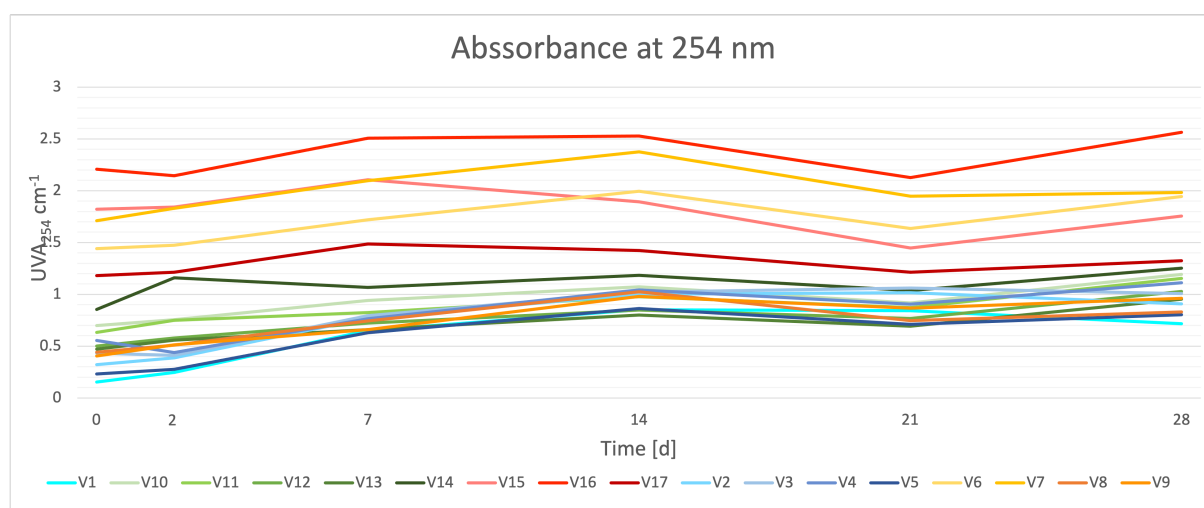


Figure 15: Timeseries of the  $UVA_{254}$  index. In general, high  $UVA_{254}$  values characterized samples with high DOC concentrations. An increasing trend was observable in all samples, even when no net-negative DOC (BDOC) was detectable. This shift in optical properties can be attributed to microbial activity in the samples.

Overall, DOC concentration was positively correlated with the  $UVA_{254}$  index (Figure 16). In general, glacier-fed streams showed a greater increase in  $UVA_{254}$  with DOC concentration (blue regression line in Figure 16). In bioassays from alpine streams at lower altitude, a comparable change in  $UVA_{254}$  required a doubling of DOC (red regression line in Figure 16). However, the  $UVA_{254}$  values, the DOC concentrations and, their relation highly depended on the sample and thus, on the geochemistry of the sampling site. This is because the  $UVA_{254}$  index is affected by the DOC concentrations and to have a better visualization of the UV absorbance and thus, the aromaticity of the water sample, it is better to normalize the index by the DOC concentration and obtain the  $SUVA_{254}$  index.

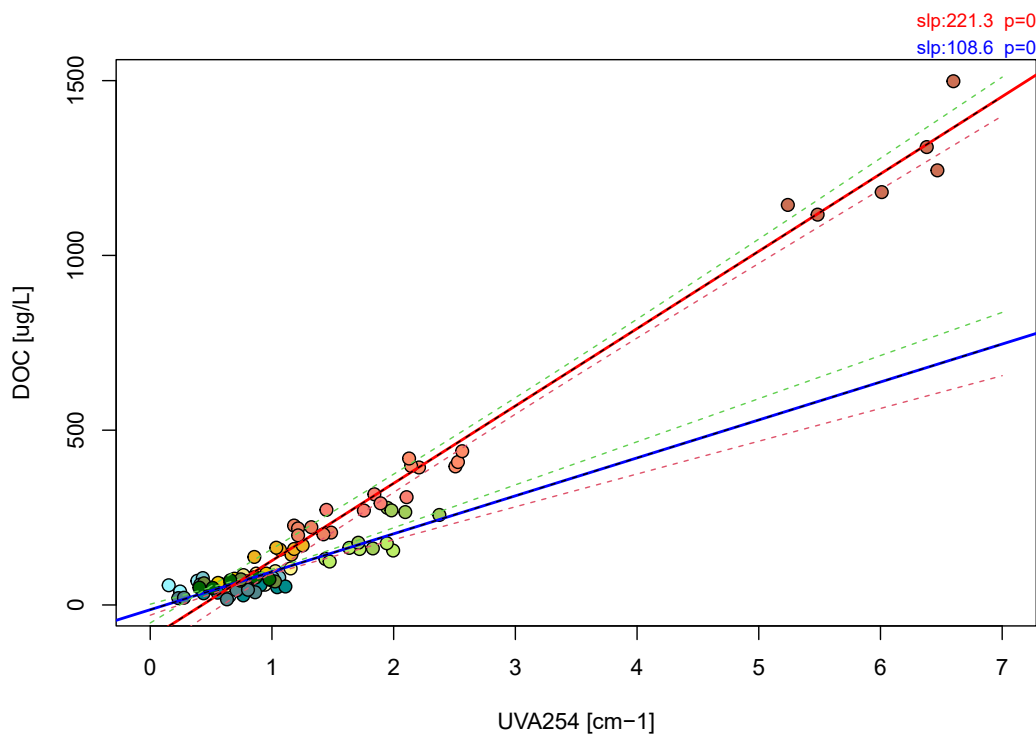


Figure 16: Regression of the DOC variability with  $UVA_{254}$ . DOC concentration was positively related to  $UVA_{254}$ , with a steeper regression line slope in the case of alpine streams at lower altitude as compared to glacier-fed streams.

$SUVA_{254}$  index timeseries are shown in Figure 17. It is noticeable that, as opposed to the  $UVA_{254}$  timeseries, the alpine streams at lower altitudes were characterized by lower  $SUVA_{254}$  values with respect to glacier-fed streams.  $SUVA_{254}$  ranged mostly between 0.005 and 0.015  $L/mg \cdot m^{-1}$ , with values that are hardly comparable with the literature due to the lack of similar studies in glacier-fed streams during winter. However, it has been found that, compared to marine systems ( $SUVA_{254}$  ranging from 0.03 ÷ 0.6  $L/mg \cdot m$ ), this index can be 10 times higher in freshwaters [37].

Moreover, at T7 a large peak is shown for samples V1, V4, and V5 and a smaller peak for samples V2 and V3. This represents an interesting feature since all of the above-mentioned samples have been taken on the same day, and in the same spatial area (Weisshorn- Matterhorn Alps on the southwest side of the Swiss Alps). Thus, it could be representative of carbon biogeochemistry (for instance the presence of aromatic compounds) related to the organic matter in that area. However, a deeper analysis should be done to better understand this pattern.

Some reviews suggest that in 1st-order streams DOM is lower in DOC concentration, less aromatic ( $SUVA_{254}$ ) and more derived from autochthonous sources with respect to higher-order streams [8]. Moreover, DOC bioavailability has been found to be negatively related to  $SUVA_{254}$  (Figure 26, Appendix B) and thus, to be higher in samples with relatively fewer aromatic compounds. Other studies have found DOC bioavailability increasing with lower  $SUVA_{254}$  [8] [19] [34] as well as more recent allochthonous DOM and more development and impervious surface [8]. However, DOM bioavailability can be both, positively and negatively correlated with  $SUVA_{254}$  in literature [8]. In general, however, DOC bioavailability variation is thought to be driven by DOC composition ( $SUVA_{254}$ ) in the case of small streams, while for large streams, inorganic nutrients were predominant in driving the DOC bioavailability [34].

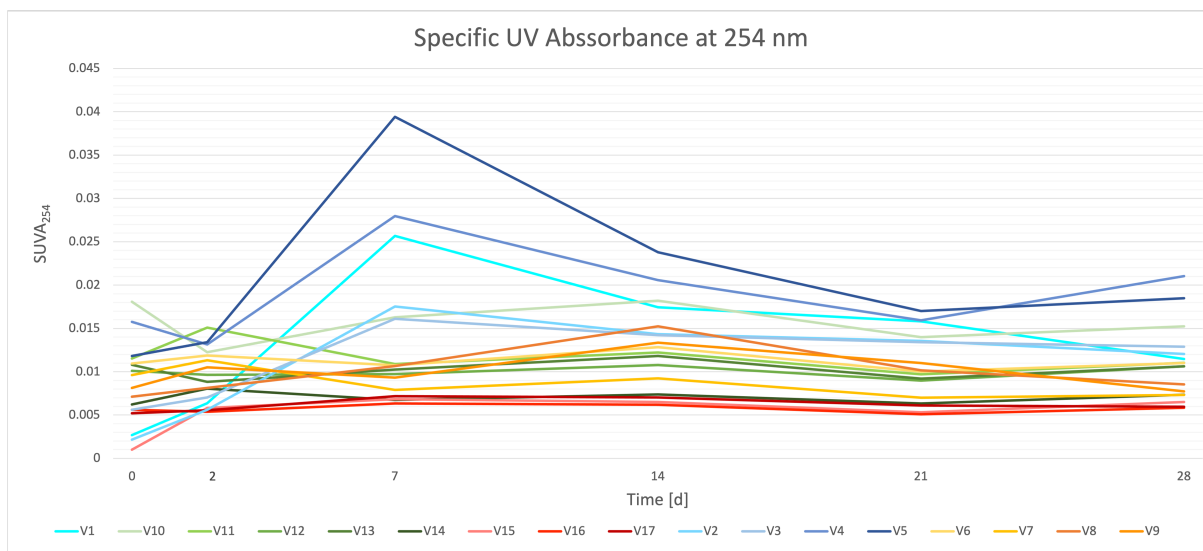


Figure 17: Timeseries of the  $SUVA_{254}$  index. The Specific UV absorbance at 254 nm is independent from the magnitude of the DOC concentration. As opposed to the  $UVA_{254}$  index, the  $SUVA_{254}$  index is higher in glacier-fed streams with low DOC concentrations. A peak of the  $SUVA_{254}$  is shown at T7 for the samples V1 to V5, all collected during the same sampling day.

#### 4.2.2 Principal Component Analysis

Principal component analysis (Figure 18) was performed with all available physico-chemical environmental parameter, dissolved ions, inorganic nutrients and *in situ* DOC (complete list in Appendix C) to identify potential drivers of net DOC change in GFS. The first principal component explained the 50.38 % of the variance while, the second principal component explained 23.85 % of the variance. Taken together, the two first components of the PCA explained 74.22 % of the variance in physico-chemical conditions in the sampled GFS.

Table 7 summarizes which variables were correlated with the principal components: the variables with the farthest number from zero in either direction are the most impacting ones. Here the correlation importance is taken for variables with an absolute value above 0.7. The first principal component (PC1) was negatively related to Calcium, Conductivity Strontium, Nitrite, Magnesium and, Sulfate. This suggests that these parameters vary together. PC1 was negatively related to Calcium (-1.066). The second principal component (PC2) was positively related to DOC and Chloride and negatively related to Sulfate (Table 7).

By looking at Figure 18, it is possible to relate the samples with the most relevant environmental parameters. Four main clusters were identified depending on the physico-chemical characteristics. The "green" cluster, on the top-left quadrant in Figure 18, contained the alpine streams at lower altitudes. In this cluster, V15 and V17 group together with high Nitrate concentrations and high pH values. V16 and, especially, V18 were marked by high *in situ* DOC concentrations as well as high Chloride and Sodium concentrations. Elevation and Potassium concentrations were low for alpine streams, but, they characterized a group of sampling sites (V6 to V9), in the central part of the Swiss Alps, together with V2 (in the western part of Switzerland). For those samples, the pH was particularly low as well as Nitrite, Sodium, Chloride, and DOC concentrations. In the bottom-left quadrant, V1, V4, and V5 clustered together and were linked to high Sulfate, Magnesium, Strontium, and Calcium concentrations and high conductivity.

The "blue" cluster on the bottom left, composed of V1, V4, and V5, was characterized by conditions potentially favoring chemolithoautotrophy. High values of inorganic nutrients, such

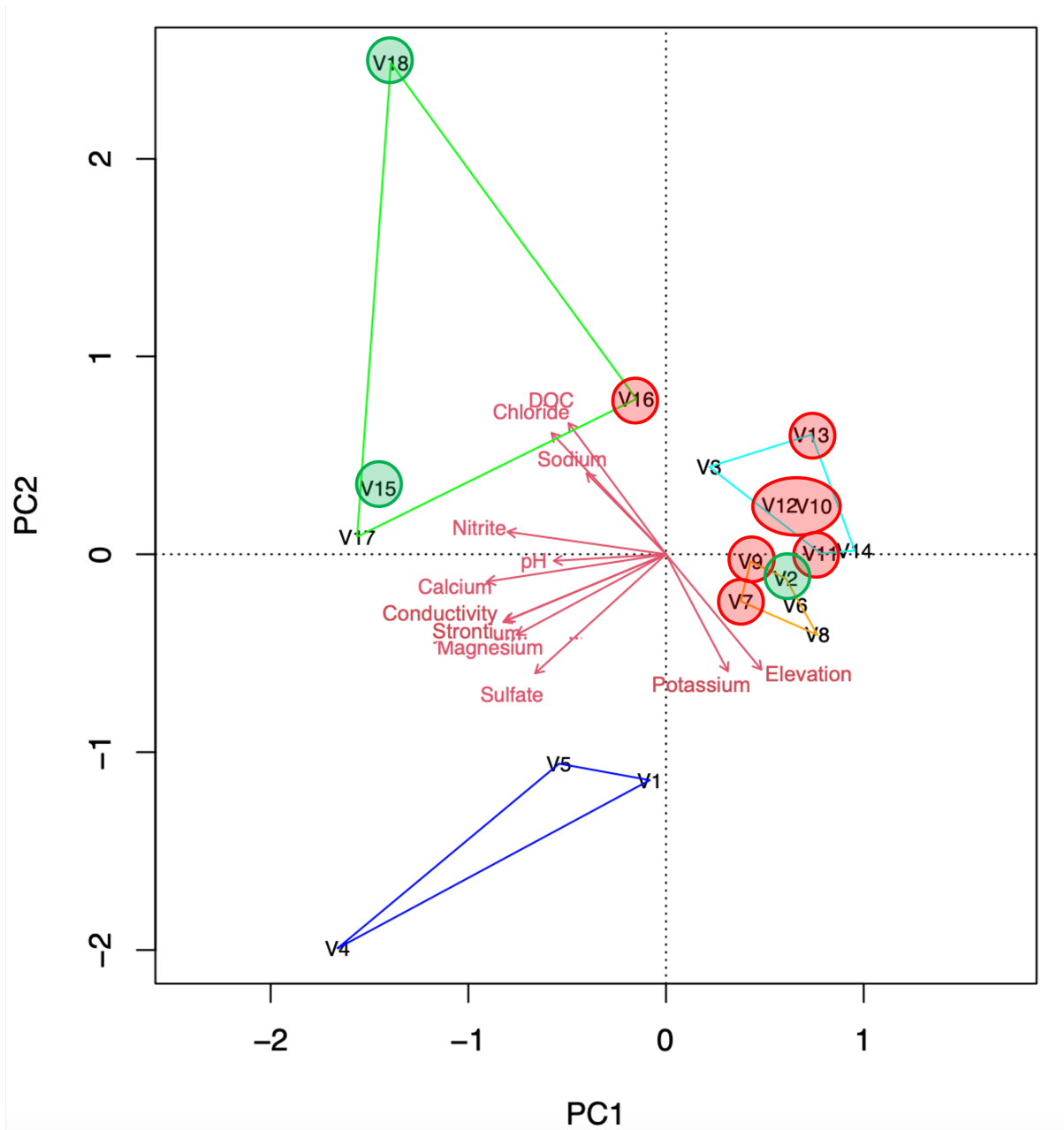


Figure 18: Principal Component Analysis: first principal component (PC1) on the x axis (50.38% explain of the variance) and second principal component (PC2) on the y axis (23.85% of the variance). Green circles highlight samples that showed net-negative DOC change (BDOC); red circles instead represent samples with a significant net positive DOC change. From this PCA, four clusters of samples can be identified. One included the alpine streams at lower altitude (from V15 to V18) and was characterized by high DOC, Chloride and Sodium concentrations. Elevated concentrations of inorganic nutrients, Sulfate, Magnesium, Strontium and Calcium that can be an index of chemolithoautotrophic favoring conditions, characterize a group of samples (V1, V4 and V5) that cluster together in the bottom-left quadrant.

Table 7: Variables correlations with the principal components (PC1 and PC2): the variables with the farthest number from zero, in either direction, are the most impacting ones. The correlation importance is taken for variables with absolute value above 0.7.

	PC1	PC2
pH	-0.668	-0.03933
Conductivity	<b>-0.9683</b>	-0.40276
Elevation	0.5674	-0.68555
Chloride	-0.6812	<b>0.72091</b>
Nitrite	<b>-0.9428</b>	0.13381
Sulfate	<b>-0.7789</b>	<b>-0.70781</b>
Sodium	-0.4729	0.48205
Magnesium	<b>-0.8892</b>	-0.47876
Potassium	0.3682	-0.69498
Calcium	<b>-1.0660</b>	-0.16281
Strontium	<b>-0.95 26</b>	-0.39389
DOC	-0.5800	<b>0.77928</b>

as Sulfate, Magnesium, and Strontium were found, however, no correlation with a significant net increase in DOC was present. Indeed, in Figure 18 the samples with net-positive DOC change ("negative" BDOC) were highlighted with a red circle and were mainly present on the opposite side of the PCA, meaning that were related to samples with low Sulfate, Magnesium, and Strontium. Samples highlighted by a green circle instead were the ones with net-negative DOC change (BDOC).

However, looking at Figure 17, the samples in the "blue" cluster (V1, V4, and V5) showed a SUVA<sub>254</sub> peak at T7 and, overall reflected higher specific UV absorbance than the other samples. Higher aromaticity could be linked to molecules that are harder to be decomposed by bacteria and, maybe, leading to lower heterotrophic bacterial activity that needs to be fueled by chemolithoautotrophic carbon production. Although they are characterized by the lower DOC concentrations of the dataset (Table 3), those samples remained within the variation range of the control sample meaning that, possibly, chemolithoautotrophic production balanced the heterotrophic carbon consumption.

### 4.3 Bacterial Abundance and Bacterial Carbon Contribution

The above-discussed DOC results were, as referred to in the previous section, representative for a net DOC balance. However, this net balance, either positive or negative, does not differentiate between the newly produced organic carbon and the one which is consumed and taken up by bacteria during the incubation period. Moreover, the samples were filtered with GF/F filters, which have a nominal pore size of  $0.7 \mu m$ , at the beginning of the incubation only. It is known from the literature that aquatic bacteria have sizes ranging in the order of the  $\mu m$  and thus they overlap the threshold between the Dissolved Organic Matter and the Particulate Organic Matter (Figure 20) [38]. Moreover, thanks to another study [36], it is known that the length of bacteria coming from glacier-fed streams in the European Alps and the Scandinavian Mountains, is mostly smaller than  $1 \mu m$  (Figure 19), meaning that potentially many bacterial cells remain in the DOC analysis.

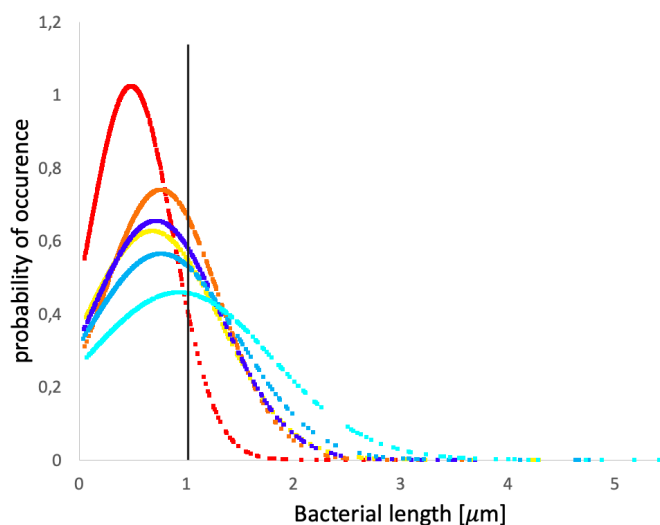


Figure 19: Probability density function of glacier-fed stream bacterial length. Figure after Ezzat et al. [36].

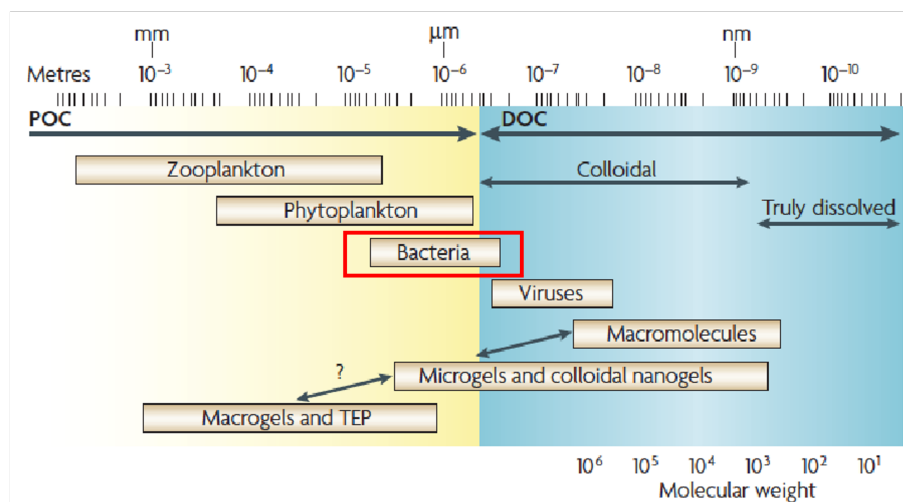


Figure 20: Bacterial size position overlaps the Dissolved Organic Carbon and Particulate Organic Carbon threshold. Image taken from Azam et Al. [38]

These bacterial cells are probably broken up during the DOC analysis of the sample due to the acid reagent injection leading to the release of their carbon content into the sample and its consequent analysis with the DOC. Thus, it is not possible to unequivocally differentiate between truly dissolved organic carbon and carbon that enters the bacterial biomass and that is then accounted for as DOC by the machine during the DOC measurement.

### 4.3.1 Bacterial Abundance

Because of that and to account for the bacterial carbon present in the samples, bacterial abundance and bacterial volume were measured and combined with a theoretical fraction of carbon present in bacterial cells. Other conversion factors, for instance based on estimates of carbon per cell are available, however, given the particularly small cell size of the bacteria in GFS, we opted for a measure that includes biovolume. The relative carbon content of cryospheric bacteria may differ from other bacteria, which may affect our results, however, no specific conversion factors are available for cryospheric bacteria. Figure 21 shows bacterial abundance (BA) for each sample at each time-step as an average of the bacterial abundance of the three replicates. Firstly, it is visible that, in all samples, bacterial abundance was low at T0 and T2, and then it rapidly increased at T7. Such a lag phase followed by exponential growth is typical for bacteria growth. After T7, bacterial abundance remained either constant or was subject to a more gradual increase.

It is noticeable that, on average, in glacier-fed streams, BA increased significantly more than in alpine streams. The reason for this could be related to the unstable sedimentary environment of GFS. In fact, rapid growth may be a key bacterial strategy to be able to colonize a constantly changing streambed environment. In line with this, previous work has found that GFS bacteria have higher number of 16S rRNA operons, a genomic trait that allows bacteria to grow rapidly [39]. Some cells can be non-growing, dormant, or inactive and it can be the case when a mismatch between total cell number and viable bacterial cells is observed [26]. Moreover, bacterial cells can be subject to lysis due to the possible development of viruses in the incubation bottles, and those cells, killed and broken up, are not accounted for by flow cytometry leading to an underestimation of total bacterial carbon content.

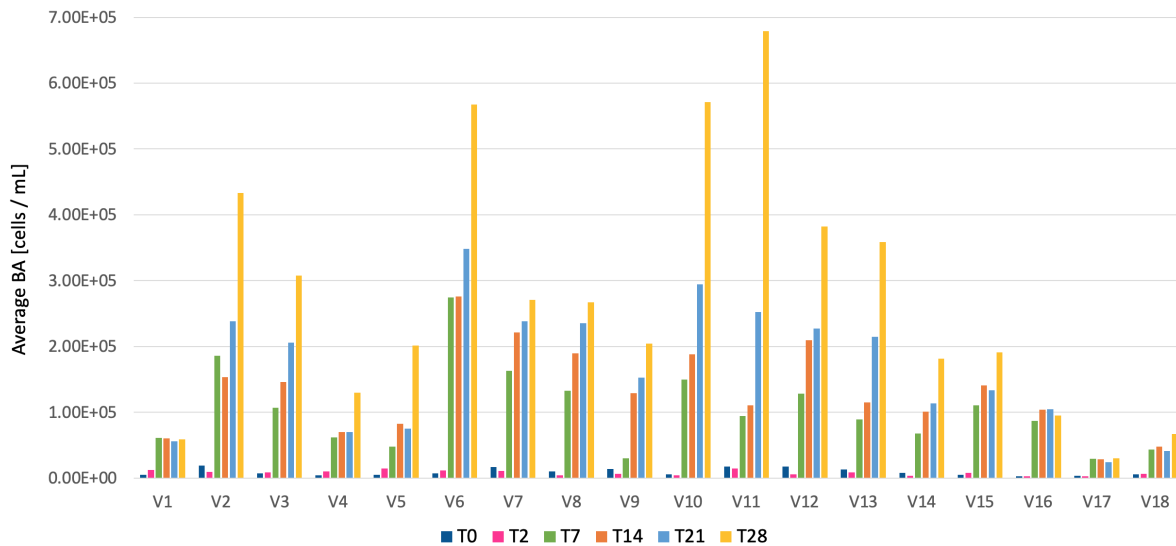


Figure 21: Average bacterial abundance [cells mL<sup>-1</sup>] for each sample, at each timestep. In all samples, BA was low at T0 and T2, then it rapidly increased at T7, remained constant or increasing gradually afterwards. The overall average BA was  $1.17 \cdot 10^5$  cells/mL.

### 4.3.2 Bacterial Volume

The bacterial carbon contribution is not only related to the number of cells present in the sample, but also to their volume. We measured bacterial cell volume at T0 for all samples to understand the average bacterial volume distribution and its variation among the samples (Figure 22). In Figure 22 it is apparent that the median value of bacterial volume was variable between samples

and similar for samples collected from the same geographical area. Cell volumes ranged from 0.05 to 0.20 [ $\mu\text{m}^3$ ], with lower values for the sites located in the central and eastern of Switzerland (i.e. V6 to V14), and larger values in the Weisshorn-Matterhorn Alps on the south-west part of the Swiss' Alps (i.e. V1 to V5). Potentially, this could be related to local geology and substrate type which may lead to different bacterial growth rates and different average bacterial volumes. However, this should be further substantiated.

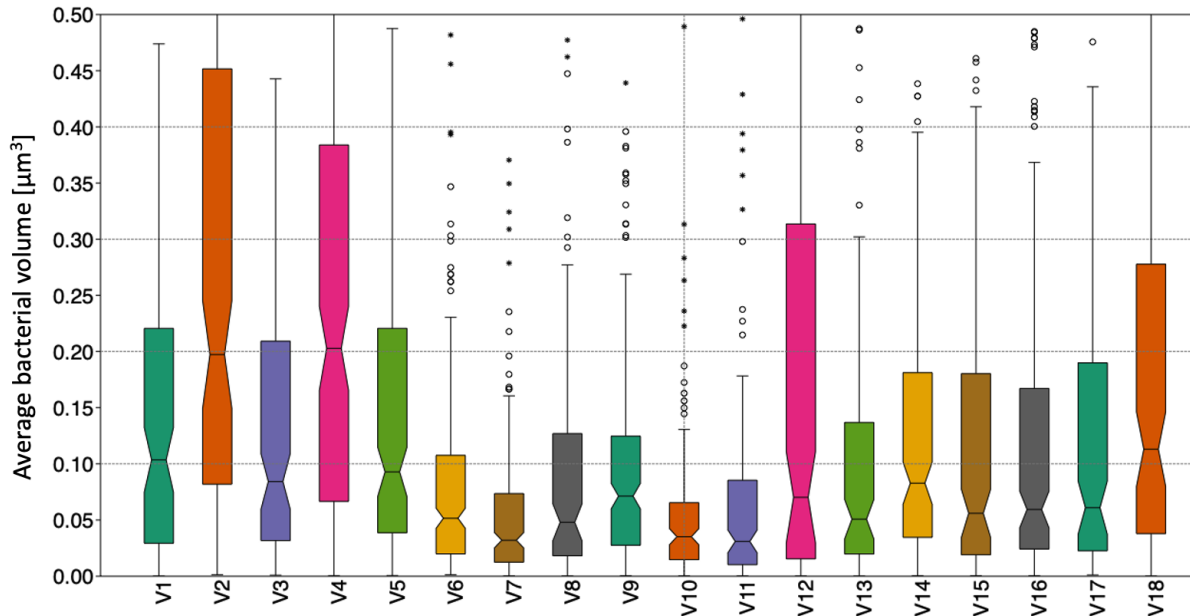


Figure 22: Boxplot of the average bacterial volume among the different samples at T0 [ $\mu\text{m}^3$ ]. For each sample, the interquartile range (IQR) is shown as a box containing all values between the 25th (Q1) and 75th (Q3) percentiles. The median value (Q2) is highlighted by an horizontal bar and a contraction of the box. Two lines, the whiskers, extending from the box, reach the minimum and maximum values given by the subtraction from Q1 or the addition to Q3 of a value corresponding to 1.5 times the IQR. The remaining dots out of this range represent potential outliers. Among the different samples, the variability of the median bacterial volume ranged between 0.05 and 0.20 [ $\mu\text{m}^3$ ] and depended on the sample. It is interesting to notice that the sample collected the same day and in the same geographical area show similar values of bacterial volume.

To understand how bacterial cell volume may change over time, bacterial volume was also measured at T14 (Figure 23a) and T28 (Figure 23b), in the exponential growth phase and stationary phase of the incubations, respectively. Because of the large effort required, however, this could only be done for selected samples, taking into account spatial and geological distribution of the samples. In some cases, such as V2 and V4 the average bacterial volume decreased, in others, like V13 and V16 it slightly increased, while in even other, V7 and V10, it increased at T14 and then decreased at T28 (Appendix D). Thus, it is not possible to identify univocal trends in average bacterial volume variation. However, the contribution to the bacterial carbon calculations, that the changes of bacterial volume among samples and in time can have, compared to the magnitude of the bacterial abundance, is considerably low. Thus, overall average bacterial volume is used for further analysis.

The average bacterial volume calculated here ranged between 0.06 and 0.48 [ $\mu\text{m}^3$ ] (Table 8), which is comparable with respect to the range 0.11 - 0.41 [ $\mu\text{m}^3$ ] found by Fagerbakke et Al. [26] for aquatic bacteria by assuming the same bacterial geometry as in this study (Figure 7).

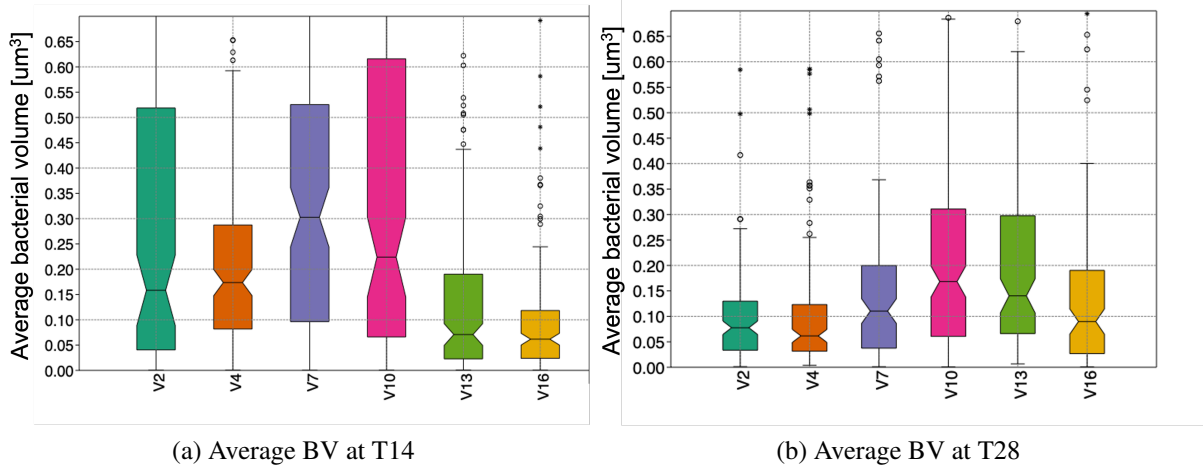


Figure 23: Boxplot of the average Bacterial Volume distribution [ $\mu\text{m}^3$ ] at T14 and T28. For each sample, the interquartile range (IQR) is shown as a box containing all the values between the 25th ( $Q1$ ) and 75th ( $Q3$ ) percentiles. The median value ( $Q2$ ) is highlighted by an horizontal bar and a contraction of the box. Two lines, the whiskers, extending from the box, reach the minimum and maximum values given by the subtraction from  $Q1$  or the addition to  $Q3$  of a value corresponding to 1.5 times the IQR. The remaining dots out of this range represent the potential outliers.

Table 8: Average Bacterial Volume [ $\mu\text{m}^3$ ] at T0, T14 and T28 for the different samples. The total average bacterial volume was found to be 0.208 [ $\mu\text{m}^3$ ].

	<b>T0</b> [ $\mu\text{m}^3$ ]	<b>T14</b> [ $\mu\text{m}^3$ ]	<b>T28</b> [ $\mu\text{m}^3$ ]	<b>Total</b> [ $\mu\text{m}^3$ ]
<b>V1</b>	0.185			
<b>V2</b>	0.342	0.476	0.097	
<b>V3</b>	0.168			
<b>V4</b>	0.298	0.213	0.105	
<b>V5</b>	0.141			
<b>V6</b>	0.090			
<b>V7</b>	0.056	0.380	0.177	
<b>V8</b>	0.133			
<b>V9</b>	0.131			
<b>V10</b>	0.065	0.409	0.243	
<b>V11</b>	0.095			
<b>V12</b>	0.179			
<b>V13</b>	0.148	0.159	0.205	
<b>V14</b>	0.197			
<b>V15</b>	0.138			
<b>V16</b>	0.128	0.127	0.174	
<b>V17</b>	0.253			
<b>V18</b>	0.190			
<b>avg</b>	0.163	0.294	0.167	0.208

### 4.3.3 Bacterial Carbon Content

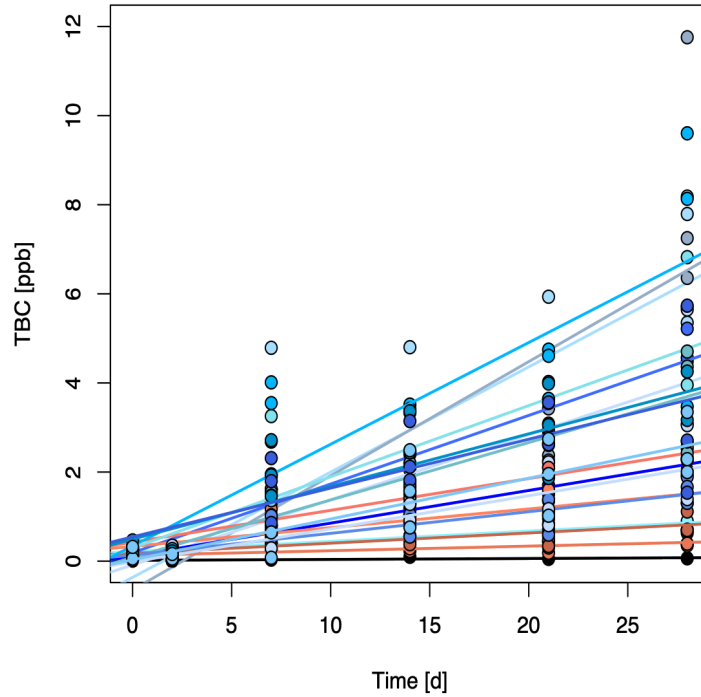


Figure 24: Bacterial Carbon Content timeseries [ppb]. Total bacterial carbon content was similar across the samples. BCC was low ( $\sim 0.1$  ppb) at  $T_0$  and slightly increased during the incubation, up to a maximum of 12 ppb. The average total bacterial carbon content was 3.5 ppb.

After the Bacterial Volume calculation and the bacterial abundance measurement, it was possible to estimate the Total Bacterial Carbon Content (TBCC). The carbon content is given by Fagerbakke et al. [26] in fg of Carbon per cell [ $\text{fg C cell}^{-1}$ ] with respect to the bacterial volume [ $\mu\text{m}^3$ ] and ranges between 7 and 31  $\text{fg C cell}^{-1}$ . In their paper [26], Fagerbakke et al., extracted a regression equation (reported in Section 3.3) which can be used to calculate average carbon content per cell. We used an average bacterial volume of 0.208 [ $\mu\text{m}^3$ ] (Table 8) and BA for all samples to calculate bacterial carbon content. Indeed, with respect to the bacterial abundance, the bacterial volume contribution to the final bacterial carbon content of the samples was four orders of magnitude lower. The average carbon content per cell was calculated to be 12.45  $\text{fg C cell}^{-1}$ , by taking the 0.208 [ $\mu\text{m}^3$ ] as average bacterial volume. Then, the average carbon content per cell was multiplied by the bacterial abundance of each replicate to obtain the

Table 9: Bacterial Carbon Content at  $T_0$  and  $T_{28}$  [ppb].

	T0	T28
<b>V1</b>	0.071	0.735
<b>V2</b>	0.303	5.389
<b>V3</b>	0.089	3.832
<b>V4</b>	0.060	1.621
<b>V5</b>	0.069	2.508
<b>V6</b>	0.093	7.068
<b>V7</b>	0.208	3.370
<b>V8</b>	0.125	3.326
<b>V9</b>	0.173	2.546
<b>V10</b>	0.084	7.109
<b>V11</b>	0.220	8.455
<b>V12</b>	0.219	4.755
<b>V13</b>	0.166	4.468
<b>V14</b>	0.099	2.262
<b>V15</b>	0.098	2.377
<b>V16</b>	0.037	1.002
<b>V17</b>	0.061	0.379
<b>V18</b>	0.059	0.837
<b>avg</b>	0.124	3.447

total average bacterial carbon present in the triplicates and subsequently, the average one in the different samples at each time step. The total bacterial carbon content obtained was similar across all samples and characterized by a very low starting values, accounting on average for merely 0.1 ppb (Table 9) at T0. The bacterial carbon present slightly increased over time for all the samples (Figure 24) and reached up to 12 ppb, at the end of the incubation, with an average across the samples of 3.5 ppb (Table 9).

To compare the magnitude of the bacterial carbon content with respect to the DOC present in the samples, in Figure 25, the DOC and TBCC timeseries are plotted for each sample individually. It is visible that the contribution of the bacterial carbon to the DOC pool of the samples was considerably small, reaching a maximum fraction of 10% of the total DOC measured.

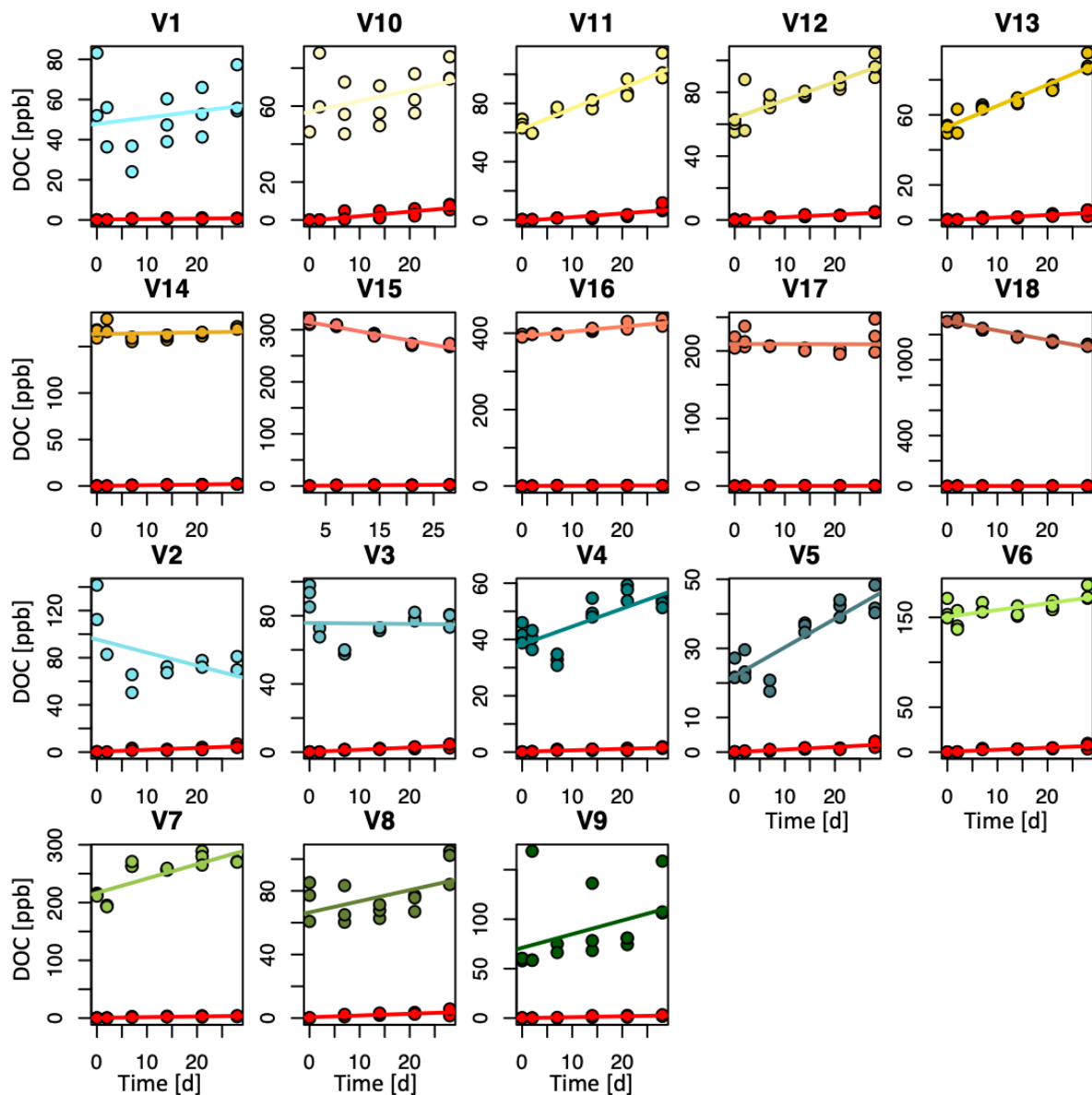


Figure 25: DOC and total bacterial carbon content timeseries [ppb]. The bacterial carbon content trend is shown in red, on the bottom of each graph and it constitutes only a small fraction of the DOC pool, never exceeding 10%.

## 5 Conclusions

In this thesis, I demonstrated that glacier-fed streams during winter are environments poor in dissolved organic carbon, as could be expected from previous research. We attribute this to the scarcity of carbon sources in GFS in winter, which were much lower as compared to streams under the tree line. The bioassay experiments revealed invariant or slight increasing DOC trends in GFS, contrasting previously reported consumption of a large fraction of bioavailable DOC in GFS. Additionally, the net increase of DOC in GFS was generally much higher than the percentage of DOC that is commonly bioavailable for bacteria as reported in the literature, in extreme cases exceeding 200% of the initial DOC concentration. Potentially, the 28 days incubation period did not allow for the observation of more significant DOC variation, especially in the case of GFSs. On the other hand, BA measurements indicated that the bacterial communities reached near-stationary phases within this time. A significant net-positive DOC change observed in some GFS samples seems to confirm the hypotheses of significant organic carbon production carried out by chemolithoautotrophic bacteria in GFS. In most cases we observed a slight increase or balance of DOC over time, indicating a balance between heterotrophic consumption and chemolithoautotrophic production of organic carbon. In fact, the coupling between chemolithoautotrophic carbon production and heterotrophic carbon consumption could be of fundamental importance for GFS ecosystems. Previous research has highlighted the role of phototrophs in structuring benthic communities in proglacial streams. However, in turbid GFS, phototrophic carbon production is limited and may be replaced by chemolithoautotrophic production. This has important consequences in light of climate change. With ongoing glacier retreat, GFS become warmer, less turbid and exhibit less pronounced diurnal variation in flow. All this may foster algal primary production and reduce the importance of chemolithoautotrophs in these unique ecosystems. We used PCA to unravel potential environmental drivers explaining DOC bioavailability dynamics. While the samples clustered in 4 distinct groups, reflecting different geology and stream characteristics, this clustering did not coincide with net-positive or net-negative DOC change measurements. In contrast, both net-positive and net-negative DOC changes instances were observable across clusters. This contrasts our hypothesis of specific GFS environments that possibly foster chemolithoautotrophic growth and hence carbon production. However, optical properties of DOM, such as high aromaticity ( $SUVA_{254}$ ), seem to be a promising avenue to better understand intrinsic DOM properties that may affect DOC bioavailability in GFS. Measurement of bacterial carbon content allowed us to distinguish between newly produced organic carbon and the one taken up by bacteria for biomass production present in the measured DOC pool. The bacterial carbon content increased during the incubation and reached a maximum of 10% of the DOC concentration. This means that the incorporation of carbon into the bacteria biomass was increasing over time, even when no net-negative DOC change evident. However, it also became apparent that TBCC does not play a crucial role in the overall DOC balance. To fully understand the carbon balances in the incubation experiments, bacterial respiration remains the challenging missing factor to account for in future research. Finally, our analyses leave space for questions regarding the reliability of the used methodology. Although much care was taken to avoid contamination, we found a similar increase in DOC in our control treatment. The source of this carbon remains unknown. To investigate in more detail the bioavailability of DOC in glacier-fed streams more research is needed. Coupled biogeochemical and molecular analyses could help to better understand the type of bacteria present and thus their role in carbon dynamics. Longer incubation could allow resolving a potential reactivity-continuum of DOC in GFS. Testing for the effects of temperature on biodegradation may add important insights on constraints of DOM degradation in GFS. Again, this could be

coupled with assays of bacterial activity and respiration. Moreover, it would also be interesting to resolve seasonal dynamics of DOM bioavailability. Here, we studied for the first time DOC bioavailability in GFS in winter, but following this up throughout the year may provide deeper insights into hot spots and hot moments of DOM degradation. Winter condition will gradually change in the future. Sites at low altitude will be affected first and will gradually shift from glacier-fed streams to mountain stream ecosystems. New carbon sources and fluxes will be imposed by the ongoing changes and not only glacier-fed streams will adapt to new conditions but also the entire fluvial system will be affected impacting the downstream life and possibly the entire food web. Understanding those changes and their impact will help understand when and where the riverine ecosystem might be a source or a sink of CO<sub>2</sub> subsequently enhancing or reducing the climate changes.

## **6 Appendices**

### **Appendix A**

List of the reagents prepared for the inorganic nutrient analysis.

**Orthophosphate Reagents:**

Ammonium Molybdate Solution  
Antimony Potassium Tartrate Solution  
Molybdate Color Reagent  
Ascorbic Acid Reducing Solution  
Sodium Hydroxide - EDTA Manifold Rinse

**Ammonia Reagents:**

Salicylate/Citrate Mixed Reagent  
Sodium Dichloroisocyanurate Reagent

**Nitrate/Nitrite and Nitrite Reagents:**

Sodium Hydroxide  
Ammonium Chloride Buffer, pH 8.5  
Sulfanilamide Color Reagent

**Digestion Reagent:**

Persulfate/Sodium Hydroxide Digesting Reagent

## Appendix B

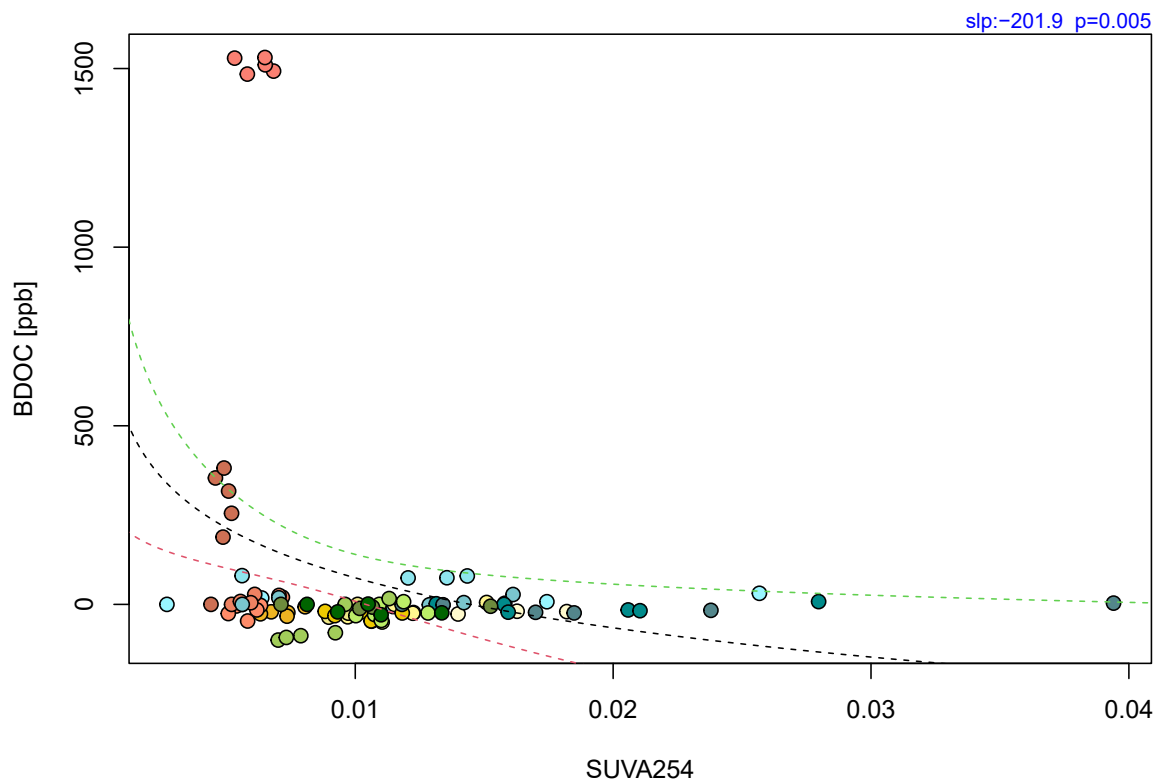


Figure 26: Logarithmic regression of the net DOC change variability with  $SUVA_{254}$ . The DOC bioavailability is negatively related to  $SUVA_{254}$  meaning that it is higher when the aromatic compounds are low.

## Appendix C

Ions [ppm]	Nutrients [ppb]	Environmental Parameters
Fluoride	PO <sub>4</sub>	Time [hours.min]
Chloride	NH <sub>4</sub>	pH
Nitrite	NO <sub>3</sub>	Conductivity [ $\mu$ S/cm]
Bromide	NO <sub>2</sub>	O <sub>2</sub> Saturation [%]
Nitrate		O <sub>2</sub> Concentration [mg/L]
Phosphate		Water Temperature [°C]
Sulfate		min CO <sub>2</sub> Concentration [ppm]
Lithium		mean CO <sub>2</sub> Concentration [ppm]
Sodium		max CO <sub>2</sub> Concentration [ppm]
Ammonium		
Magnesium		
Potassium		
Calcium		
Strontium		

Nutrients in GFSs:

NO<sub>3</sub>: 864±756.3 [ $\mu$ g/L = ppb]

NH<sub>4</sub>: 17±8.3 [ $\mu$ g/L = ppb]

Literature values for nutrients of GFSs in the Swiss Alps [27]:

NO<sub>3</sub>: 615±203.6 [ $\mu$ g/L = ppb]

NH<sub>4</sub>: 18.1±9.6 [ $\mu$ g/L = ppb]

## Appendix D

Small changes in the average bacterial volume of sample V4 between T0 and T14 (Figure 27a and 27b) are reflected in the microscope images (Figure 28a and 28b). It is visible that the bacteria's size is almost the same at the two observed timesteps, only the spatial distribution varies, with a more spread and even distribution of the cells on the filter at T0 (Figure 28a) in comparison with a tendency to aggregate at T14 (Figure 28b).

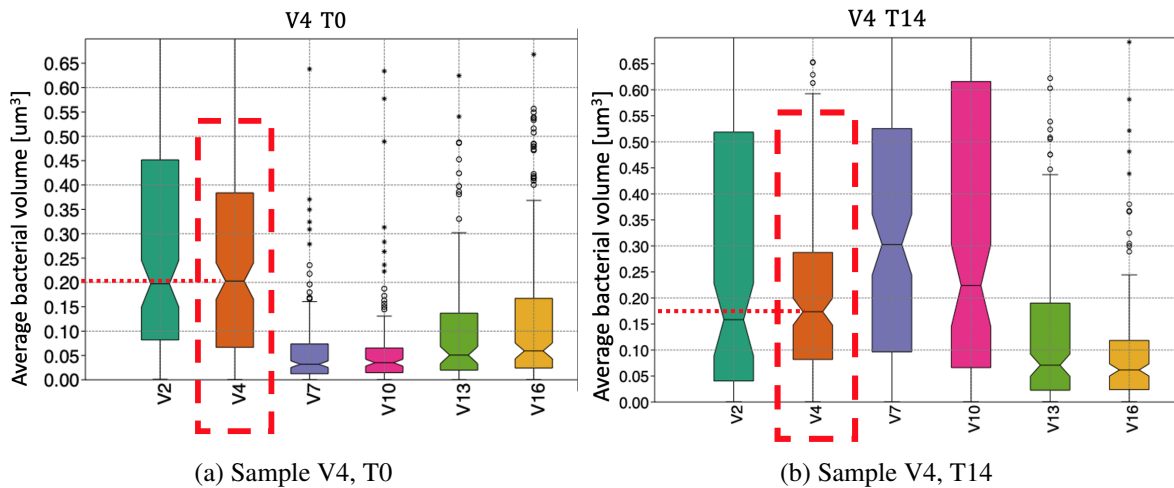


Figure 27: Change of the average bacterial volume of V4 between T0 and T14.

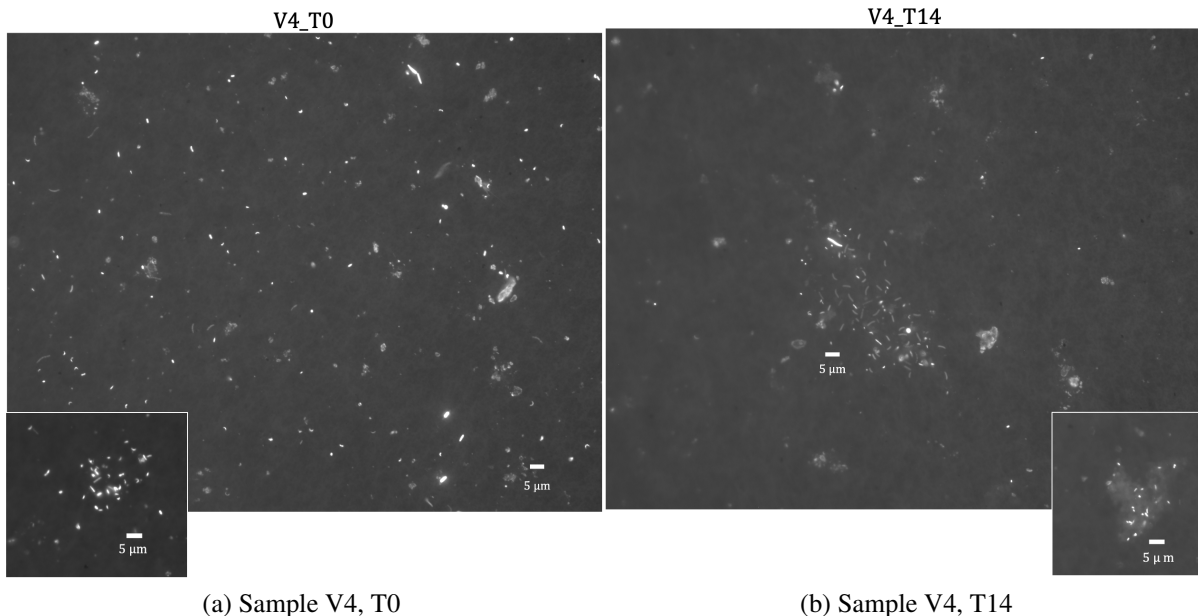


Figure 28: Microscope images of the bacteria in sample V4 at T0 and T14.

On the other side, for sample V10, the average bacterial volume at T14 (Figure 29a) increases five times with respect to T0 (Figure 29b). It is visible in the microscope images that the cells are really small at T0 (Figure 30a) and surrounded by some noise (particles present in the sample), while at T14 (Figure 30b), the cells are fat and really well visible.

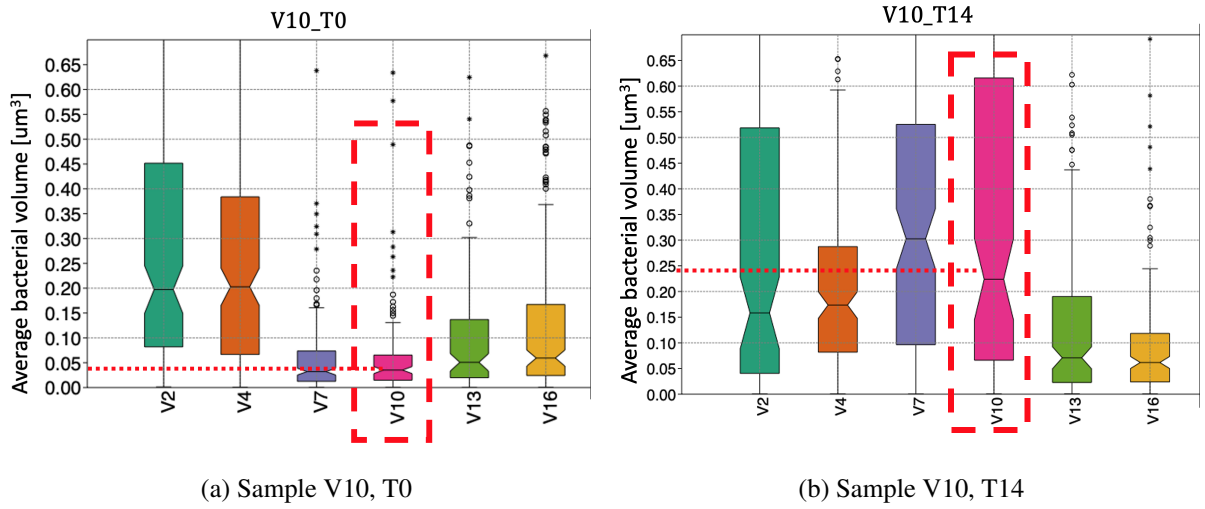


Figure 29: Change of the average Bacterial Volume of V4 between T0 and T14.

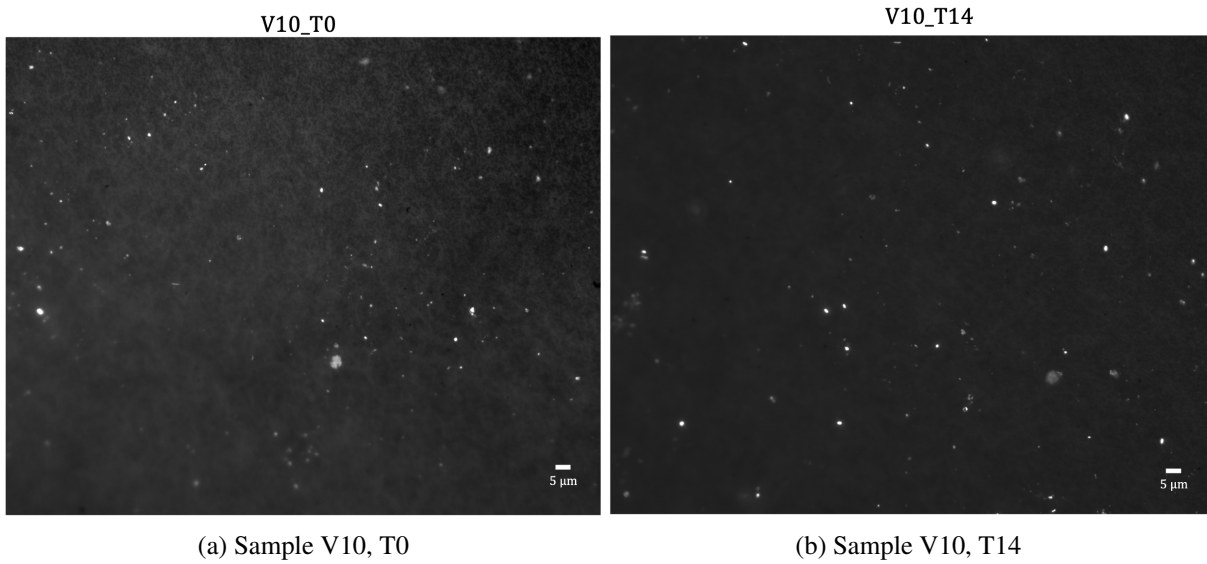


Figure 30: Microscope images of the bacteria in sample V10 at T0 and T14.

## Appendix E

List of images from the sampling campaign.





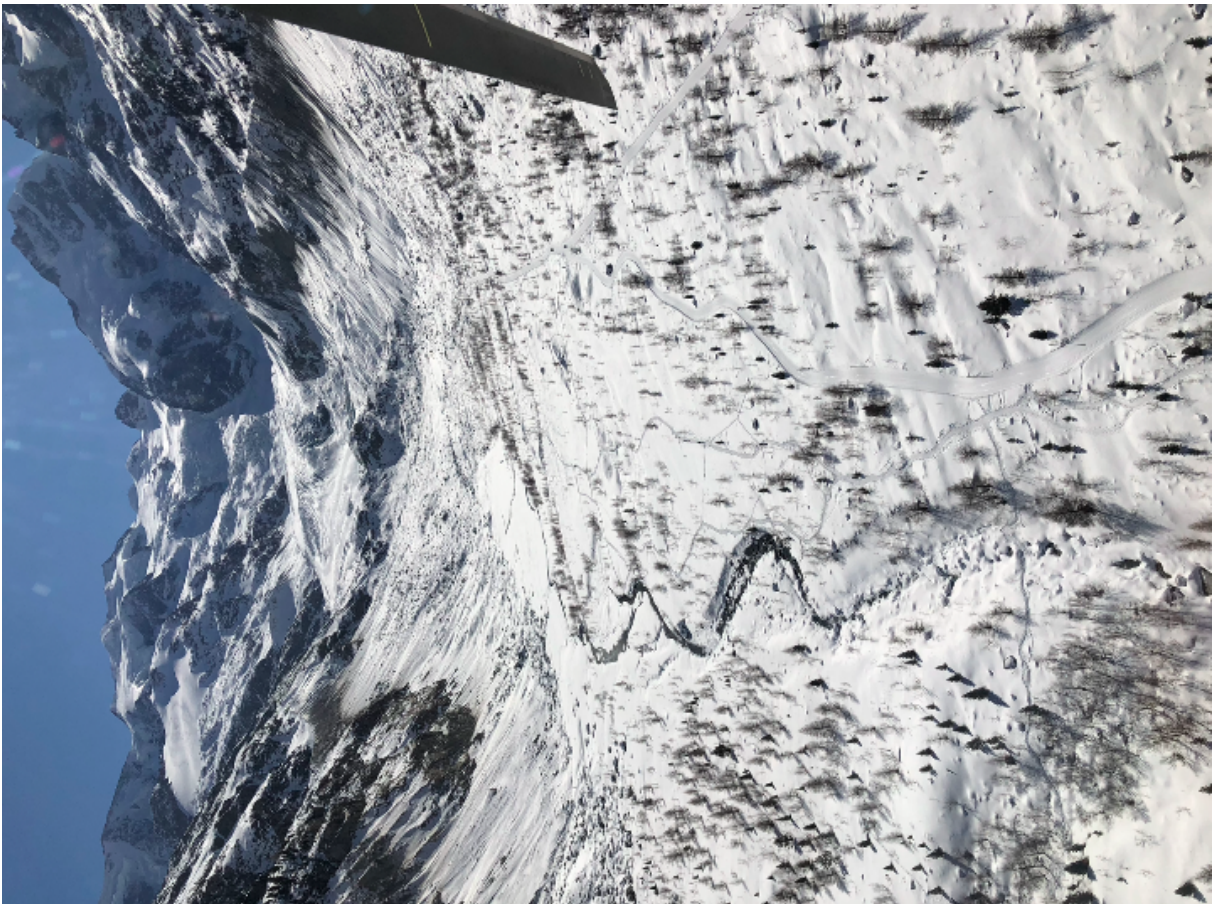
























## 7 Bibliography

### References

- [1] Battin T.J., Luysaert S., Kaplan L.A., Aufdenkampe A.K., Richter A., Tranvik L.J., The boundless carbon cycle. *Nature Geosci* 2, 598–600. (2009). <https://doi.org/10.1038/ngeo618>
- [2] Findlay S., Sinsabaugh R.L., Unravelling the sources and bioavailability of dissolved organic matter in lotic aquatic ecosystems. *Marine and Freshwater Research* 50, 781-790. (1999). <https://doi.org/10.1071/MF99069>
- [3] Singer G.A., Fasching C., Wilhelm L., Niggemann J., Steier P., Dittmar T., Battin T.J., Biogeochemically diverse organic matter in Alpine glaciers and its downstream fate. *Nature Geosci* 5, 710–714. (2012). <https://doi.org/10.1038/ngeo1581>
- [4] Hosen J.D., McDonough O.T., Febria C.M., Palmer M.A., Dissolved Organic Matter Quality and Bioavailability Changes Across an Urbanization Gradient in Headwater Streams. *Environmental Science Technology* 48 (14), 7817-7824. (2014). <https://doi.org/10.1021/es501422z>
- [5] Dodds W.K., Whiles M.R., Aquatic Chemistry and Factors Controlling Nutrient Cycling: Redox and O<sub>2</sub>. In *Aquatic Ecology, Freshwater Ecology (Second Edition)*, 12, 289-321. (2010). <https://doi.org/10.1016/B978-0-12-374724-2.00012-X>
- [6] Weishaar J.L., Aiken G.R., Bergamaschi B.A., Fram M.S., Fujii R., Mopper K., Evaluation of Specific Ultraviolet Absorbance as an Indicator of the Chemical Composition and Reactivity of Dissolved Organic Carbon. *Environmental Science Technology*, 37 (20), 4702-4708. (2003). <https://doi.org/10.1021/es030360x>
- [7] Casas-Ruiz J.P., Spencer R.G.M., Guillemette F., Von Schiller D., Obrador B., Podgorski D.C., Kellerman A.M., Hartmann J., Gómez-Gener L., Sabater S., Marcé R., Delineating the continuum of dissolved organic matter in temperate river networks. *Global Biogeochemical Cycles*, 34. (2020). <https://doi.org/10.1029/2019GB006495>
- [8] Coble A.A., Wymore A.S., Potter J.D., McDowell W.H., Land Use Overrides Stream Order and Season in Driving Dissolved Organic Matter Dynamics Throughout the Year in a River Network. *Environmental Science Technology*, 56 (3), 2009-2020. (2022). <https://doi.org/10.1021/acs.est.1c06305>
- [9] Vonk J.E., Tank S.E., Mann P.J., Spencer R.G.M., Treat C.C., Striegl R.G., Abbott B.W., Wickland K.P., Biodegradability of dissolved organic carbon in permafrost soils and aquatic systems: a meta-analysis. *Biogeosciences*, 12, 6915–6930. (2015). <https://doi.org/10.5194/bg-12-6915-2015>
- [10] Battin T.J., Kaplan L.A., Findlay S., Hopkinson C.S., Marti E., Packman A.I., Newbold J.D., Sabater F., Biophysical controls on organic carbon fluxes in fluvial networks. *Nature Geosci* 1, 95–100. (2008). <https://doi.org/10.1038/ngeo101>
- [11] Thi Mai Huong Nguyen, Thi Phuong Quynh Le, Vinh Van Hoang, Da Le Nhu, Cam Tu Vu, Duong Thi Thuy, Seasonal and spatial variation in biodegradability of organic carbon along the Red River, Vietnam. *Carbon Management*, 12:5, 549-557. (2021). <https://doi.org/10.1080/17583004.2021.1980110>
- [12] Kolka R., Weishampel P., Fröberg M., Measurement and Importance of Dissolved Organic Carbon. Hoover, C.M. (eds) *Field Measurements for Forest Carbon Monitoring*. (2008). [https://doi.org/10.1007/978-1-4020-8506-2\\_13](https://doi.org/10.1007/978-1-4020-8506-2_13)
- [13] Servais P., Anzil A., Ventresque C., Simple Method for Determination of Biodegradable Dissolved Organic Carbon in Water. *Applied and Environmental Microbiology*, (1989). <https://doi.org/10.1128/aem.55.10.2732-2734.1989>
- [14] Pontiller B., Martínez-García S., Lundin D., Pinhassi J., Labile Dissolved Organic Matter Compound Characteristics Select for Divergence in Marine Bacterial Activity and Transcription. *Frontiers in Microbiology*, 11. (2020). <https://doi.org/10.3389/fmicb.2020.588778>

- [15] Hansen A.M., Kraus T.E.C., Pellerin B.A., Fleck J.A., Downing B.D., Bergamaschi B.A., Optical properties of dissolved organic matter (DOM): Effects of biological and photolytic degradation. *Limnology and Oceanography*, 61 (3), 1015-1032. (2016). <https://doi.org/10.1002/lno.10270>
- [16] Textor S.R., Guillemette F., Zito P.A., Spencer R.G.M., An Assessment of Dissolved Organic Carbon Biodegradability and Priming in Blackwater Systems. *JBR Biogeosciences*, 123, 2998-3015. (2018). <https://doi.org/10.1029/2018JG004470>
- [17] Mostovaya A., Hawkes J.A., Koehler B., Dittmar T., Tranvik L.J., Emergence of the Reactivity Continuum of Organic Matter from Kinetics of a Multitude of Individual Molecular Constituents. *Environmental Science Technology*, 51 (20), 11571-11579. (2017). <https://doi.org/10.1021/acs.est.7b02876>
- [18] Lambert T., Perolo P., Escoffier N., Perga M., Enhanced bioavailability of dissolved organic matter (DOM) in human-disturbed streams in Alpine fluvial networks. *Biogeosciences*, 19, 187-200. (2022). <https://doi.org/10.5194/bg-19-187-2022>
- [19] Wickland k.P., Aiken G.R., Butler K., Dornblaser M.M., Spencer R.G.M., Striegl R.G., Biodegradability of dissolved organic carbon in the Yukon River and its tributaries: Seasonality and importance of inorganic nitrogen. *Global Biogeochemical Cycles*, 26. (2012). <https://doi.org/10.1029/2012GB004342>
- [20] Anesio A.M., Hodson A.J., Fritz A., Psenner R., Sattler B., High microbial activity on glaciers: importance to the global carbon cycle. *Global Change Biology*, 15 (4), 955-960. (2009). <https://doi.org/10.1111/j.1365-2486.2008.01758.x>
- [21] Eiler A., Evidence for the Ubiquity of Mixotrophic Bacteria in the Upper Ocean: Implications and Consequences. *Applied and Environmental Microbiology*, 72 (12). (2006). <https://doi.org/10.1128/AEM.01559-06>
- [22] Enrich-Prast A., Bastviken D., Crill P., Chemosynthesis. *Encyclopedia of Inland Waters* (1), 211-225. (2009). <https://doi.org/10.1016/B978-012370626-3.00126-5>
- [23] Fodelianakis S., Washburne A.D., Bourquin M., Pramateftaki P., Kohler T.J., Styllas M., Tolosano M., De Staercke V., Schön M., Busi S.B., Brandani J., Wilmes P., Peter H., Battin T.J., Microdiversity characterizes prevalent phylogenetic clades in the glacier-fed stream microbiome. *ISME J* 16, 666-675. (2022). <https://doi.org/10.1038/s41396-021-01106-6>
- [24] Busi S.B., Bourquin M., Fodelianakis S., Michoud G., Kohler T.J., Peter H., Pramateftaki P., Styllas M., Tolosano M., De Staercke V., Schön M., De Nies L., Marasco R., Daffonchio D., Ezzat L., Wilmes P., Battin T.J., Genomic and metabolic adaptations of biofilms to ecological windows of opportunity in glacier-fed streams. *Nat Commun* 13, 2168. (2022). <https://doi.org/10.1038/s41467-022-29914-0>
- [25] The Cambrian Foundation, Chemolithoautotrophic bacteria. <http://cambrianfoundation.org/chemolithoautotrophic-bacteria/>
- [26] Fagerbakke K.M., Heldal M., Norland S., Content of carbon, nitrogen, oxygen, sulfur and phosphorus in native aquatic and cultured bacteria. *Aquatic Microbial Ecology* 10, 15-27. (1996). <https://doi.org/10.3354/ame010015>
- [27] Boix Canadell M., Gómez-Gener L., Ulseth A.J., Cléménçon M., Lane S.N., Battin T.J., Regimes of primary production and their drivers in Alpine streams. *Freshwater Biology*, 66 (8), 1449-1463. (2021). <https://doi.org/10.1111/fwb.13730>
- [28] Vannote R.L., Minshall G.W., Cummins K.W., Sedell J.R., Cushing C.E., The River Continuum concept. *Canadian Journal of Fisheries and Aquatic Sciences*, 37, 130-137. (1980). <https://doi.org/10.1139/f80-017>
- [29] Elham Kazemi, Saiedeh Razi Soofiyani, Hossein Ahangari, Shirin Eyvazi, Mohammad Saeid Hejazi, Vahideh Tarhriz, Chemolithotroph Bacteria: From Biology to Application in Medical Sciences. *Crescent Journal of Medical and Biological Sciences*, 8 (2), 81-89. (2021). [https://www.cjmb.org/uploads/pdf/pdf\\_CJMB\\_481.pdf](https://www.cjmb.org/uploads/pdf/pdf_CJMB_481.pdf)

- [30] Fellman J.B., Hood E., Raymond P.A., Hudson J., Bozeman M., Arimitsu M., Evidence for the assimilation of ancient glacier organic carbon in a proglacial stream food web. *Limnology and Oceanography*, 60 (4), 1118-1128. (2015). <https://doi.org/10.1002/lno.10088>
- [31] Boix Canadell M., Escoffier N., Ulseth A.J., Lane S.N., Battin T.J., Alpine glacier shrinkage drives shift in dissolved organic carbon export from quasi-chemostasis to transport limitation. *Geophysical Research Letters*, 46, 8872–8881. (2019). <https://doi.org/10.1029/2019GL083424>
- [32] Tranter M., Sharp M.J., Lamb H.R., Brown G.H., Hubbard B.P., Willis I.C., Geochemical weathering at the bed of Haut Glacier d’Arolla, Switzerland—a new model. *Hydrological Processes*, 16, (5), 959-993. (2002). <https://doi.org/10.1002/hyp.309>
- [33] Wauthy M., Rautio M., Christoffersen K.S., Forsström L., Laurion I., Mariash H.L., Peura S., Vincent W.F., Increasing dominance of terrigenous organic matter in circumpolar freshwaters due to permafrost thaw. *Limnol Oceanogr Lett*, 3, 186-198. (2018). <https://doi.org/10.1002/lol2.10063>
- [34] Futing Liu, Dong Wang, Dissolved organic carbon concentration and biodegradability across the global rivers: A meta-analysis. *Science of The Total Environment*, 818. (2022). <https://doi.org/10.1016/j.scitotenv.2021.151828>
- [35] Federal Office of Topography swisstopo, COGIS (Coordination, Geoinformation and Services ). Data: [swisstopo.map.geo.admin.ch](https://swisstopo.map.geo.admin.ch)
- [36] Ezzat L., Fodelianakis S., Kohler T.J., Bourquin M., Brandani J., Busi S.B., Daffonchio D., De Staercke V., Marasco R., Michoud G., Oppliger E., Peter H., Pramateftaki P., Schön M., Styllas M., Tadei V., Tolosano M., Battin T.J., Benthic Biofilms in Glacier-Fed Streams from Scandinavia to the Himalayas Host Distinct Bacterial Communities Compared with the Streamwater. *Applied and Environmental Microbiology*, 88 (12). (2022). <https://doi.org/10.1128/aem.00421-22>
- [37] Deflandre B., Gagné JP., Estimation of dissolved organic carbon (DOC) concentrations in nanoliter samples using UV spectroscopy. *Water Res*, 35(13), 3057-62. (2001). [https://doi.org/10.1016/s0043-1354\(01\)00024-0](https://doi.org/10.1016/s0043-1354(01)00024-0)
- [38] Azam F., Malfatti F., Microbial structuring of marine ecosystems. *Nat Rev Microbiol* 5, 782–791. (2007). <https://doi.org/10.1038/nrmicro1747>
- [39] Niederdorfer R., Besemer K., Battin T.J., Peter H., Ecological strategies and metabolic trade-offs of complex environmental biofilms. *npj Biofilms Microbiomes* 3, 21. (2017). <https://doi.org/10.1038/s41522-017-0029-y>